Study on physical measures against subsequent sediment flow following debris flow deposition in high population density area

(人口密集地域における土石流後続流の

対策工法についての研究)

Hokkaido University

Graduate School of Agriculture

Yongrae KIM

CONTENTS

List of Tables

List of Figures

Abstract

There are many areas where subsequent sediment flow (sediment flow following debris flow deposition at sabo dam, hereinafter ″SSF″) flows down and disaster occurs to residential areas. SSF can cause damage to buildings, property, and human life, as well as the local economy. Typical countermeasures against SSF following debris deposition include channel works and sand pockets; however, these measures require extensive open areas. Therefore, alternative countermeasure designs must be considered for residential areas with high population density. The objective of this study is to propose a novel SSF countermeasure for installation at sabo facilities upstream of residential areas.

1. Actual situation and characteristic of damaged area from subsequent sediment flow in Hiroshima City

In order to clear the actual situation of damage due to SSF in high population density areas, the survey was conducted in Hiroshima City where damaged from SSF by torrential rain in 2018 (4 sites).

In study sites, the only countermeasure against SSF was drainage but the allowable discharge of drainage was insufficient to control the discharge of SSF. Therefore damages to houses were confirmed; broken windows and walls, sediment inflows, flooded the garden, and, etc. This result shows why alternative countermeasures in residential areas must be considered.

2. Experimental study of physical measures against subsequent sediment flow following debris flow deposition by the sabo dam

2.1 Combined application of the SSF breaker, polymer, and sub-dam

Three types of debris capture facilities were installed (SSF breaker, polymer, and sub-dam) to investigate their effects singly and in combination. Simulated debris flow was trapped by the sabo dam model, and SSF was controlled by the three countermeasures installed downstream of the dam. Sediment was separated from water using the SSF breaker and then trapped by the sub-dam.

Sediment volume decreased and elapsed time increased as the sediment flowed through the experimental countermeasure structures, leading to dramatic reductions in peak discharge and sediment concentration (over 90%) downstream of the sabo dam. The most effective value of ratio of mean particle diameter (on SSF breaker) to SSF breaker opening size is 0.54 in this study.

2.2 Combined application of the SSF breaker, 2nd SSF breaker polymer, and sub-dam

The following flume experiment was conducted by adding 2nd SSF breaker on sub-dam to previous experiment condition in order to capture more sediment from SSF. Sediment was separated from water twice using SSF breaker and 2nd SSF breaker before trapped by the sub-dam.

SSF mitigated effectively mitigated as in the previous experiments. Sediment concentration was reduced 32 ~ 80% as capture the sediment from SSF by 2nd SSF breaker when compared with the previous experiments. The effect of polymer couldn′t

be verified clearly in both of flume experiments because very short periods were allowed for gelation by the polymer during experiments.

The novel SSF countermeasure proposed in this experiment can reduce the sediment concentration and hydrograph scale of the SSF. As a result, it is expected that the extent of flooding and sedimentation of the SSF in high population density areas can be reduced, and damage to house, especially the damage caused by sand and water intrusion into house due to the destruction of opening can be reduced.

Chapter 1

General Introduction

High population density areas located in debris flow prone area can be seriously damaged when debris flow occur. On 27 July 2011, debris flows occurred by extreme rainfall in Korea (Umyeonsan, Seoul and Majeoksan, Chuncheon). These resulted in a total of 16 fatalities and 13 fatalities, also serious damage to houses, roads, and other properties [*Jeong et al.*, 2015]. Likewise, On 20 August 2014, several debris flows occurred in Hiroshima, Japan. These resulted in also 74 fatalities and serious damage to the residential area [*Doshida and Araiba*, 2015] (Fig. 1-1). Furthermore disasters has been reported in many places [*Mizuyama and Ishikawa*, 1989; *Dahal et al.*, 2009; *Miwa and Taketoshi*, 2018], and continues to occur. These disasters show the necessity of sufficient erosion control works in debris flow prone areas in order to mitigate damage.

Fig. 1-1. Photographic of damaged from SSF
(A: Umyeonsan, Korea, B: Majeoksan, Korea, C: Hiroshima, Japan)

In the Japanese sabo dam system, a single dam is generally constructed at a valley outlet to capture debris flow in regions prone to torrential rainfall. New standards for sabo dam design were proposed by the National Institute for Land and Infrastructure Management (NILIM) in 2016, highlighting the need to empirically and theoretically estimate the amount of debris flow that might accompany extreme rainfall events, characterized by 100-year exceedance probability for 24-hour or daily rainfall. Several studies have reported the effects of sabo dams in mitigating debris flow damage by trapping sediment [*Senoo et al.*, 1983; *Irazawa and Shimohigashi*, 1988; *Ohkubo et al.*, 1988] (Fig. 1-2.).

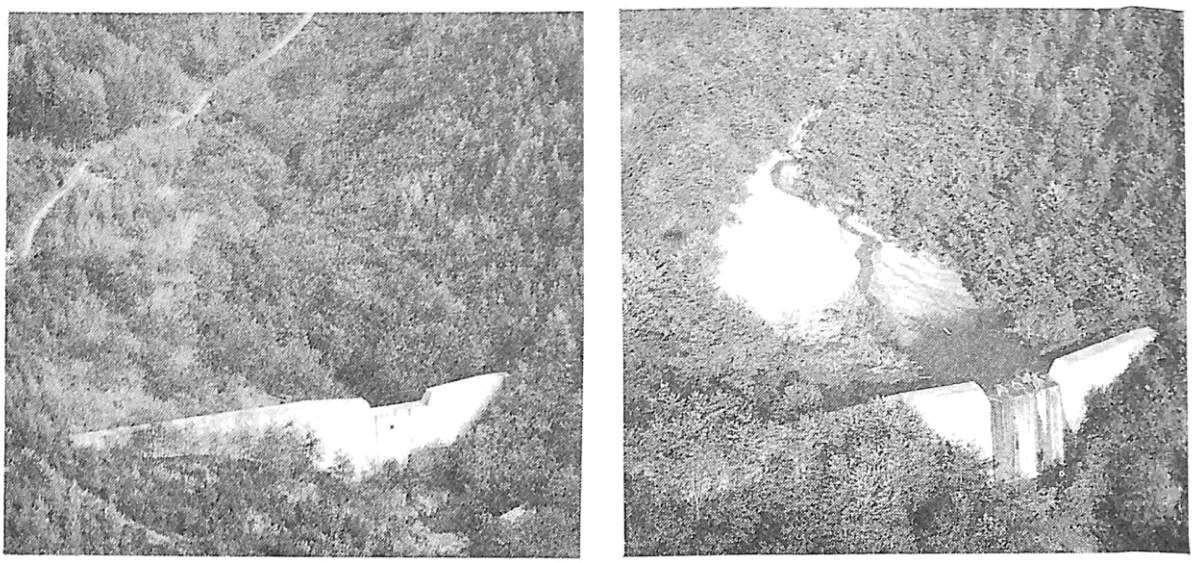

Fig. 1-2. Function of SD (Closed type)
(Irazawa and Shimohigashi,1988)

However, despite SDs are constructed, there are many areas where debris flow flows down and disaster occurs. SDs have their trapping capacity of effectively trap the debris flow. When SD loses trap capacity, SDs can not trap enough sediment to reduce the debris flow [*Mizuyama et al.,* 1998] and causes disasters at downstream. There are basically two types of disasters in these areas. SD trapped the debris flow, and then sediment flow flows to downstream in the lower of SD. Whereas, part of debris flow overflow through SD and deposit on downstream directly in the lower of SD in case debris flow volume is larger than SD designated capacity. And after, sediment flow flows to downstream. Phenomenon of mentioned first, it defines as a subsequent sediment flow (hereinafter "SSF") in this study (Fig. 1-3). Here, the sediment concentration of SSF is lower than debris flow, < 40% [*Pierson*, 2005]. SSF may reach residential areas, and such events can cause damage to buildings, property, and human life, as well as the local economy. Also we recognized the actual situation of damaged by SSF where disaster occurred at Hiroshima in 2018 (Fig. 1-4.).

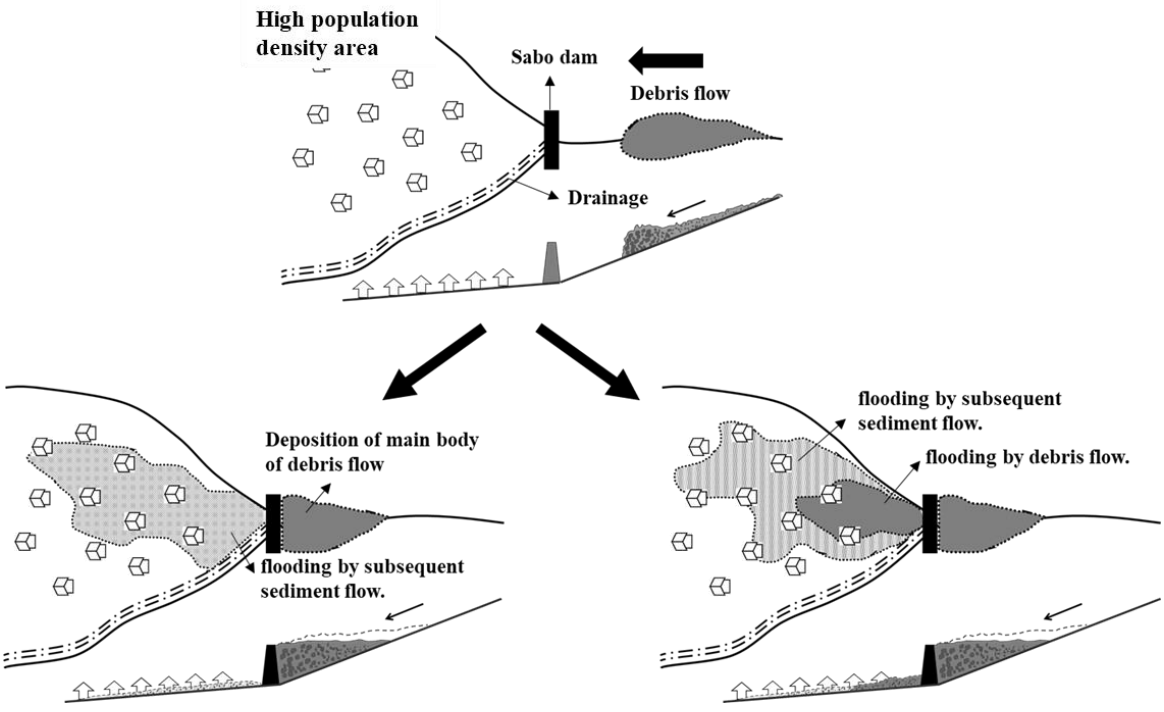

Fig. 1-3. Generation and kinds of SSF

Fig. 1-4. Trace of damage from SSF

Therefore, countermeasure against SSF are sometimes installed downstream of sabo dams such as channel works or sediment basin (Fig. 1-5). Also, *Marchi et al.* [2019] mentioned construction of channel works is need for sediment transport and protecting residential area. However, such countermeasures require extensive open areas and are therefore difficult to construct near high population density area (Fig. 1-6). Therefore the small scale of drainage located in downstream of SD, but the cross-sectional area of drainage be insufficient to control the SSF (Fig. 1-7). For these reasons, the Japan Society of Erosion Control Engineering (JSECE) emphasized the necessity of installing SSF countermeasures in residential areas following the 2018 Hiroshima disaster [*JSECE*, 2015].

Fig. 1-5. Countermeasures against the SSF
(Left: Channel works, Right: Sediment basin)

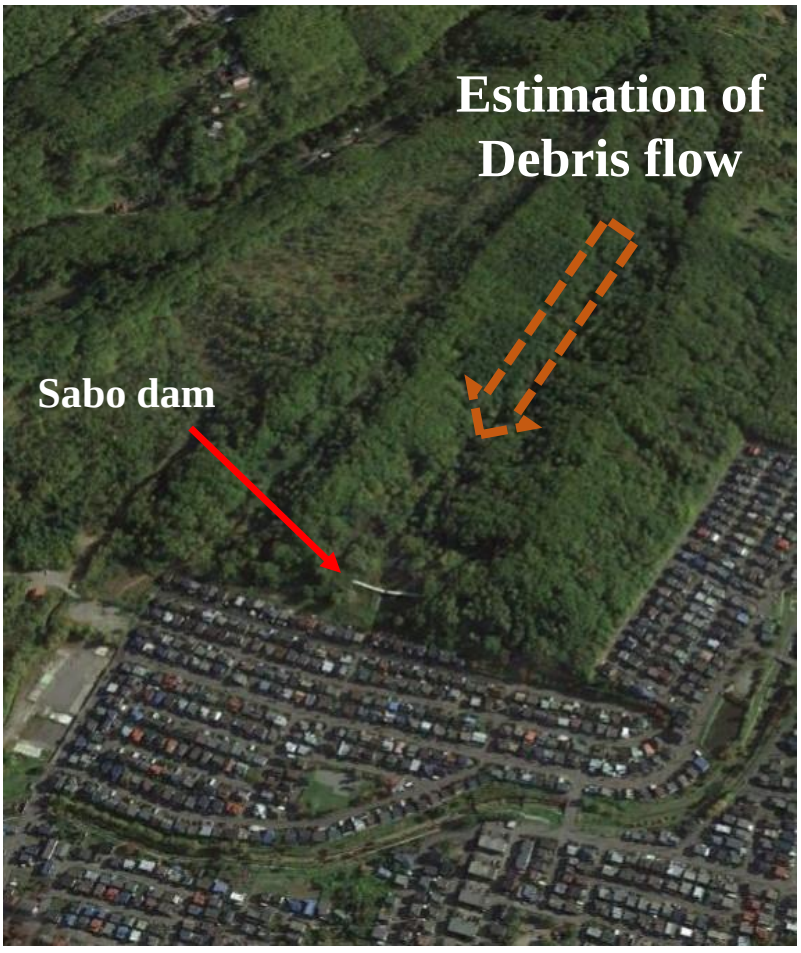

Fig. 1-6. High population density area without SSF countermeasures

Fig. 1-7. Insufficient scale of drainage (Hiroshima, Japan)

On September 2008, debris flow occurred in Ibigawa, Gifu, Japan. Although SD and channel works were constructed in this area, SSF caused damage to downstream residential area. The damage was caused by obstructing the flow of SSF at the road which was across the channel works (Fig. 1-8). The scale of channel works was insufficient to control the SSF due to the lack of space because the residential area was located downstream. This case shows that SSF needs to be mitigated before it flows into the residential area.

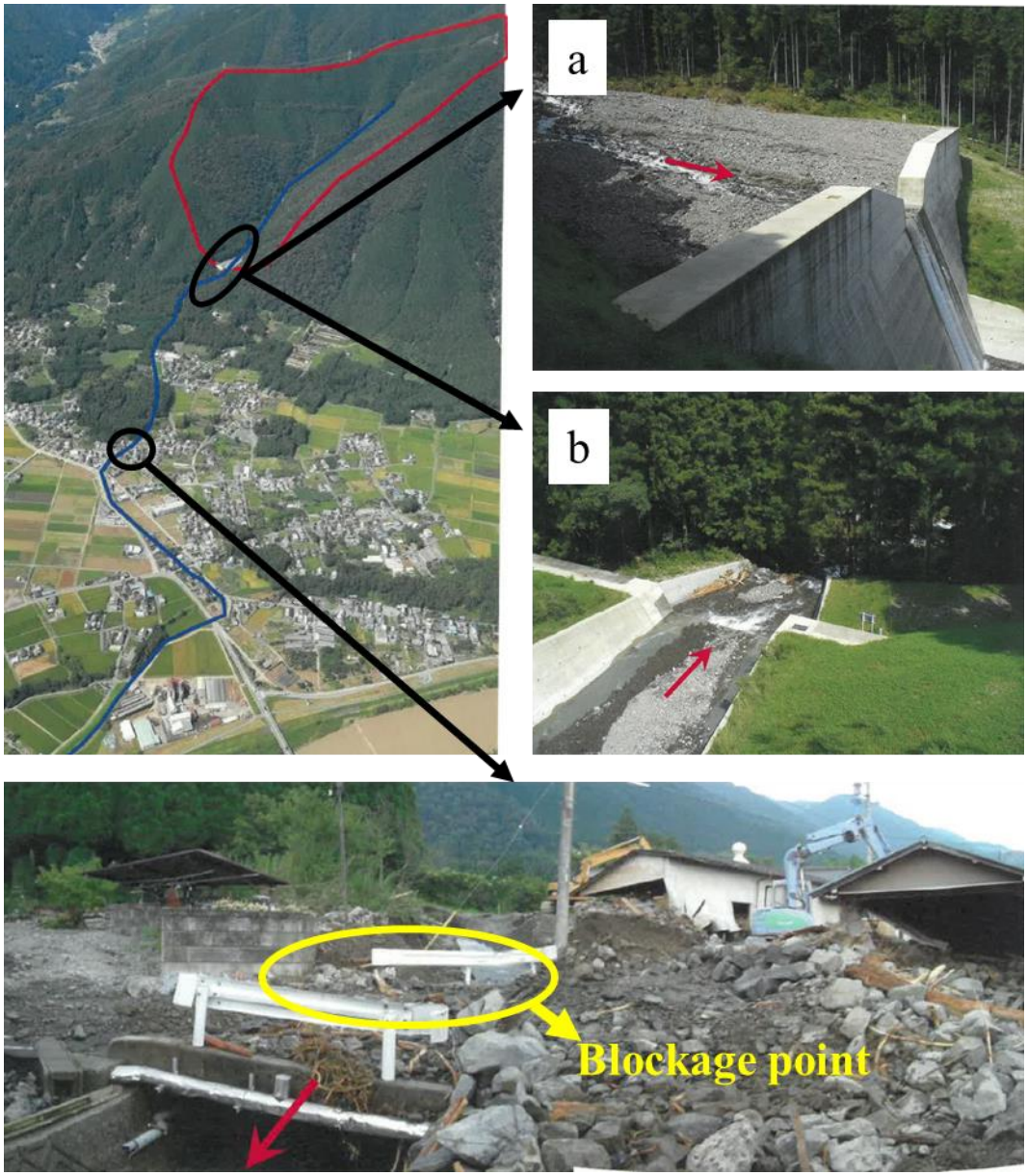

Fig. 1-8. Photographic of damaged area (Ibigawa, Japan)

To mitigate SSF, outflow discharge and sediment concentration must be reduced by separating sediment from water. Open dams, including grid sabo dam, slit sabo dam, flexible barrier or wire net, and debris flow breaker [*Mizuyama*, 2008; *Takahara and Matsumura*, 2008; *Volkwein et al.*, 2011; *Brighentia et al.*, 2013; *Brunkal and Santi*, 2016], are a typical structure to separate sediment from debris flow. Among them, debris flow breakers are one of the structures to prevent sediment-related disasters by separate sediment and water in mountain terrains and residential areas [*ICHARM*, 2008]. *Watanabe et al*. [1980] has shown that the capturing effect of debris flow (mud) by debris flow breaker, and separation of water and sediment by debris flow breaker was filmed in Mt. Yakedake [*Kiyono et al.*, 1986; *Imai et al.*, 1989] (Fig. 1-9). The mechanisms of this process have been previously explained [*Gonda*, 2009], and quantitative and qualitative assessments have been performed using a flat-board SSF breaker [*Kim et al.*, 2016]. This type of countermeasure is thus effective for the separation of water and sediment as long as the size of the breaker openings is narrower than the debris flow. Similarly, a water–sediment separation structure was recently proposed to remove coarse particles from debris flow [*Xie et al.*, 2014, 2017]; it consisted of a drainage dyke, herringbone water–sediment separation grid, outflow channel, and deposit field. This structure was found to reduce the discharge of debris flow; however, sediment flow after separation was not controlled. The flow of water and fine sediments must be further mitigated downstream of the breaker to prevent damage.

Water-absorbing polymer is considered an efficient material for controlling the flow of water in SSF due to the polymer's gelation properties. Flume experiments using such polymers have demonstrated their ability to mitigate debris flow [*Arai et al.*, 1997; *Kurihara et al.*, 1989]. Fine sediment could be further controlled by the installation of a sub-dam downstream of these measures.

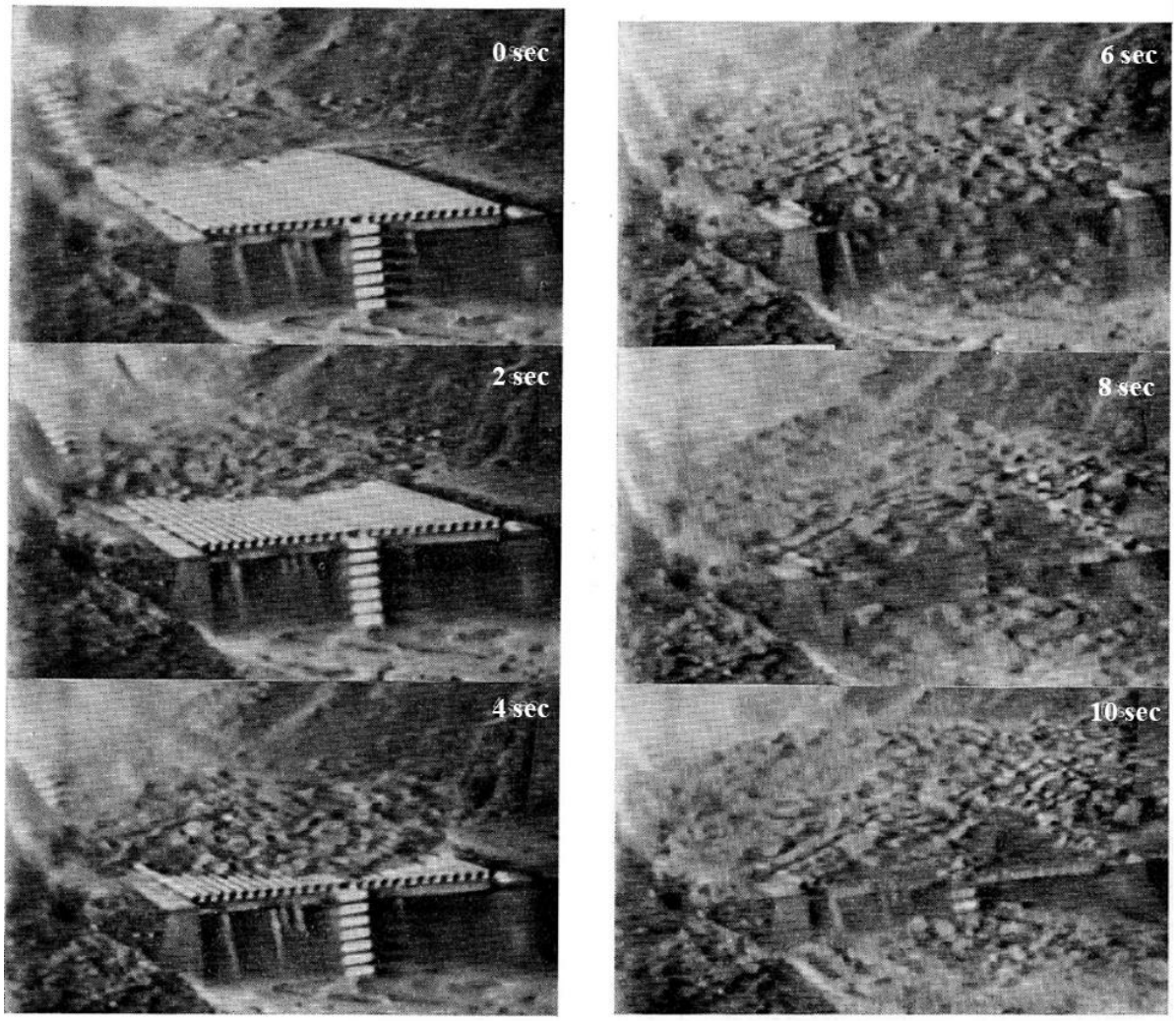

Fig. 1-9. Sequential pictures of debris flow on debris breaker in Mt. Yakedake (*Kiyono et al.*, 1986)

Consequentially, hydrodynamic force and impact force of SSF will reduce by the mitigating process of the SSF. Several studies analyzed the impact force of debris flow to sabo dam or buildings as a damaging factor [*Yamamoto et al.*, 1998; *Cui et al.*, 2015; *Zeng et al.*, 2015; *Cho et al.*, 2016;*Song et al.*, 2018]. However, the impact force changes depending on the shape or material of building, grain size in flow, etc. In case new structures, it can be constructed with considering less impact force. Nevertheless, this study is targeting the residential area which already located. Therefore in order to reduce damage to residential areas from SSF, it is necessary to mitigate the SSF by reducing the hydrodynamic force.

Many previous studies researched how to mitigate or prevent debris flow. *Kasai* [1980], *Iverson* [1997], *Kasim et al.* [2016], and others researched about characteristics of debris flow. *Shrestha et al.* [2008], *Iverson*, [2015], and others conducted experimental study to understanding of behavior and mechanism of debris flow. *Takahashi et al.* [2001], *Hubl et al.* [2005], and others reported effect of debris flow countermeasures. And, *Ishikawa et al.* [2016] and *Hiramatsu et al*. [2017] reported subsequent debris flow which movement by rainfall in interval after debris flow occurred before. However this subsequent debris flow is different with SSF targeted in this study. Any researches have not been reported about SSF yet.

The objective of this thesis was to propose a novel SSF countermeasure for installation at sabo facilities upstream of high population density areas. We investigated physical measures against SSF that are applicable in narrow areas by performing flume experiments using models of three types of SSF countermeasures (SSF breaker, polymer, and sub-dam) to examine their effects on SSF discharge and duration. In addition, in order to decrease more concentration as trap the sediment which dropped from SSF breaker, following flume experiment was conducted by adding 2nd SSF breaker on sub-dam (Fig. 1-10).

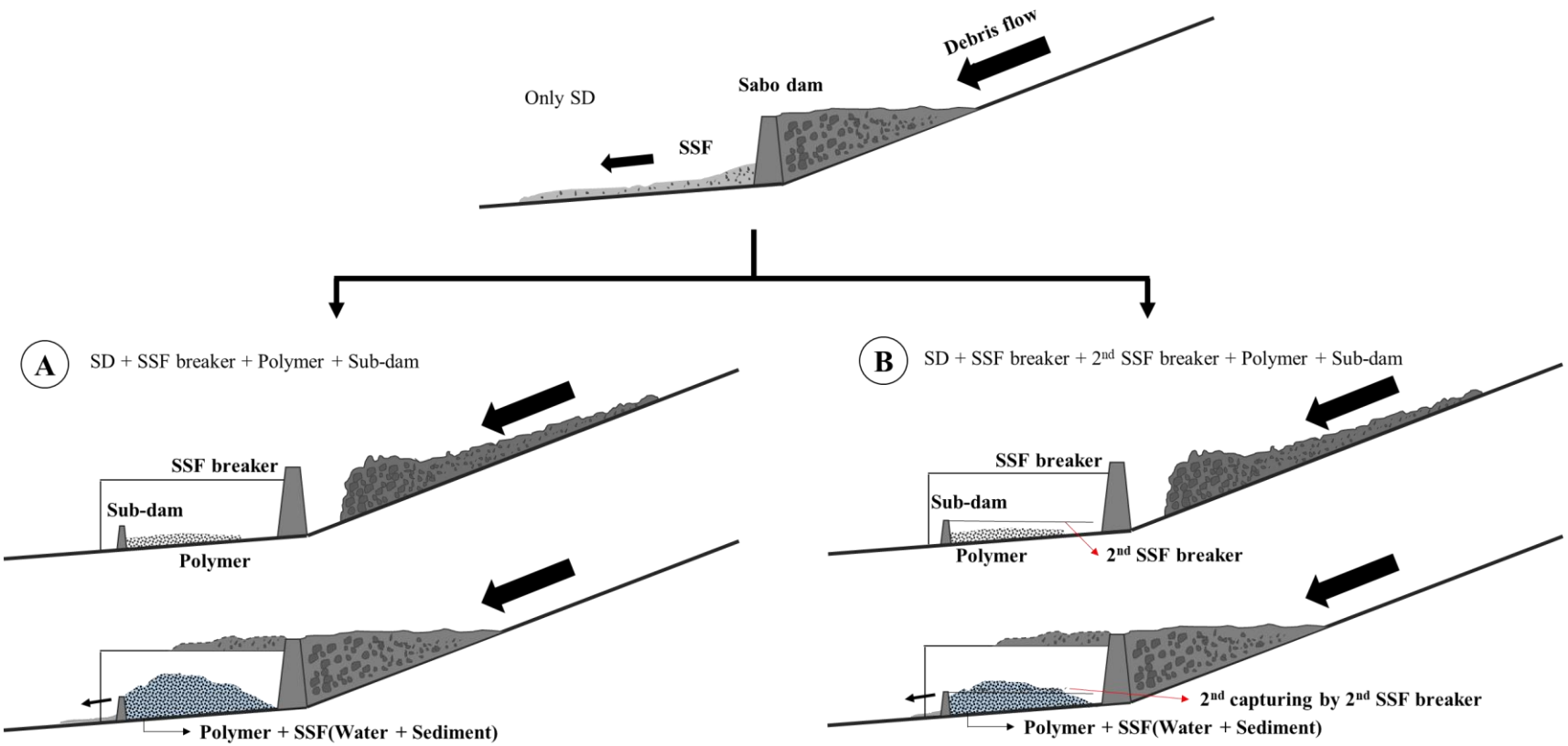

Fig. 1-10. SSF mitigate conception

(A: combined application of the SSF breaker, polymer, and sub-dam,

B: combined application of the SSF breaker, 2nd SSF breaker, polymer, and sub-dam)

Chapter 2

Structure of the thesis

SSF can occur in any debris flow prone area. If there is a high population density area in downstream, the SSF gives damage. Chapter 3 conducted a field survey of the damaged Hiroshima area from SSF in July 2018 to confirm the actual situation. A total of 4 sites were selected for field survey using aerial photographs of the Geospatial Information Authority of Japan and reports from local government. In the field survey, the discharge and the hydraulic force of SSF were calculated to identify the characteristics of the SSF. The allowable discharge of drainage in each survey site was also calculated to confirm that if it had been possible to control the SSF.

In order to reduce such damages, the construction of channel works or sediment retarding basin is required as SSF countermeasures. Those countermeasures are needed extensive area. However, construction is difficult in high population density areas due to not enough space because of land use such as houses or roadway. Through field surveys, we identify the necessity for new countermeasures for SSF in high population density area and propose new methods for mitigating SSF. It is important to reduce the hydrograph in order to mitigate the SSF. Chapter 4 and 5 identifies the mitigation of the SSF through a flume experiment.

In chapter 4, the results were expected to mitigating SSF by adding experimental countermeasure structures (SSF breaker, polymer, and sub-dam) to SD. Attached the SSF breaker to the SD to decrease the peak discharge and concentration of SSF by separating sediments from the SSF. And place the polymer under the SSF breaker to absorb the water after separation. At the last step, in order to trap the sediments of SSF and create a pool for increasing the absorption ability of polymer, a sub-dam is installed. To confirm the mitigation of the SSF through the flume experiment, the peak discharge, concentration and elapsed time were measured to draw a hydrograph of SSF.

In chapter 5, a 2nd SSF breaker is attached to the sub-dam to enhance the effectiveness of

the experimental countermeasure structures reducing SSF that proposed in chapter 4. SSF breaker catch the sediment of SSF first and then again catch the sediment from falling SSF by 2nd SSF breaker.

Through the flume experiments, clear the effect of proposed SSF countermeasures by decreasing concentration and peak discharge of SSF, also lower hydrograph of SSF. However, this study is just the indoor experiment step so far. In the flume experiment, the amount of supplied sediment and water was fixed. However, in the field, the characteristics of the runoff sediment are also different depending on the characteristics of the basin. Therefore it should be considered some considerations in order to apply to the field.

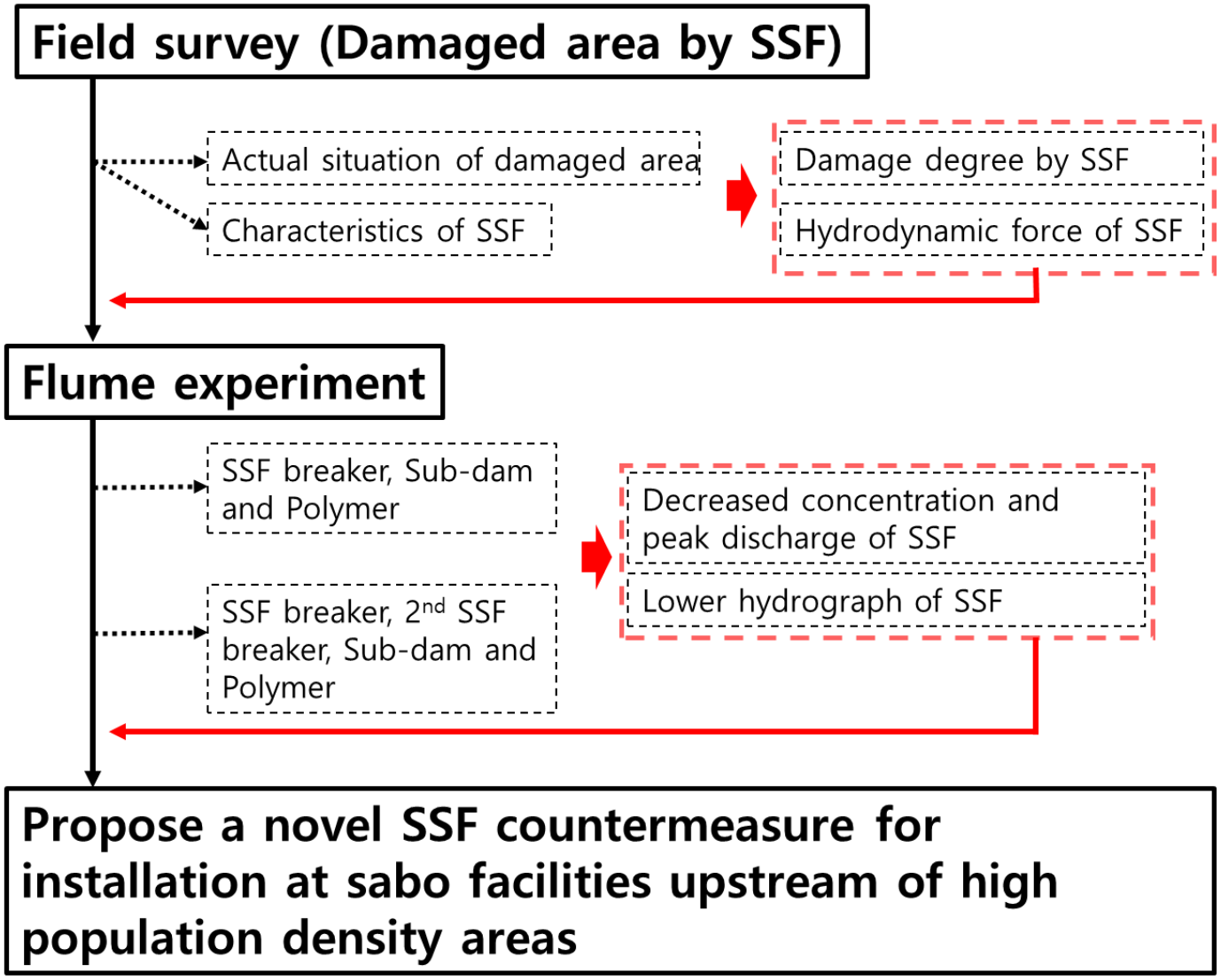

Figure 2-1. Flow chart of the thesis

Chapter 3

Actual situation of damaged area from Subsequent Sediment Flow in Hiroshima

3.1 Introduction

In Hiroshima, there is population of more than 2.8 million and also has a high population on debris flow hazard zone. Therefore many countermeasures for debris flow are constructed. However, debris flow occurred in 487 places by torrential rainfall in July 2018. Many houses were damaged and 87 people were killed due to debris flow [*Hiroshima prefecture*, 2018]. Some areas have been damaged due to absence or breakage of the countermeasures, but some areas have been affected by the SSF which is targeting in this study. As mentioned in the Introduction section, channel works or sand pocket is necessary in high population density area against the SSF. The damaged areas were high population areas without channel works or sand pocket. Because it is not easy to construct the countermeasures against to SSF in high population density area because of land uses. Already roadways or houses are located at the downstream of the valley. Also, even if there is drainage in downstream, allowable discharge of drainage may insufficient to control the SSF. Hence the study on the effective countermeasures against the SSF in high population density areas is necessary. We surveyed 4 places which was damaged by the SSF to figure out the characteristics and actual situation of SSF.

3.2 Method

3.2.1 Study sites

To confirm the necessity of the countermeasures for SSF in high population density areas, the field survey was conducted in Hiroshima. Study sites were 4 places, places were determined that high population density areas had damaged from SSF even

though sabo dam was constructed at outlet of the valley (Fig. 3-1). The red dotted lines in each study site's aerial photograph show the flooded area by SSF. These ranges were confirmed through aerial photography and field survey.

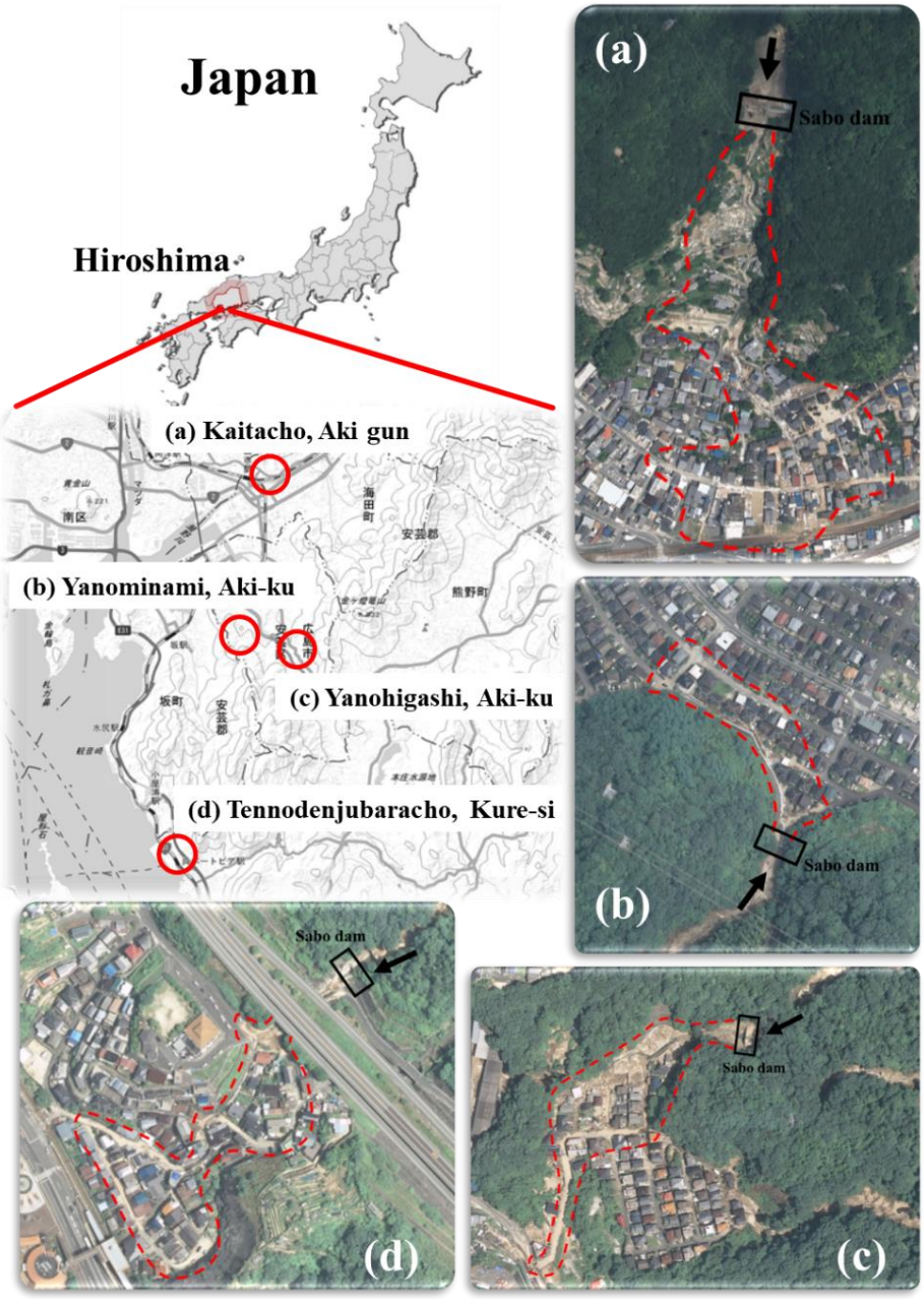

Fig. 3-1. Study sites in Hiroshima ((a) Kaitacho, Aki-gun, (b) Yanominami, Aki-Ku, (c) Yanohigashi, Aki-Ku, (d) Tennodenjubaracho, Kure-si)

3.2.1.1 Kaitacho, Aki Gun

Fig. 3-2 shows aerial photograph and actual situation of Kaitacho, Aki Gun. In the lower of SD, there is a drainage on the left side and grave area on the right side. And many houses in the downstream. Due to such these land uses, it seemed impossible to construct the countermeasures against SSF. SSF mainly flowed along the road and sediment inflows to houses or glass breakage were surveyed (Fig. 3-3).

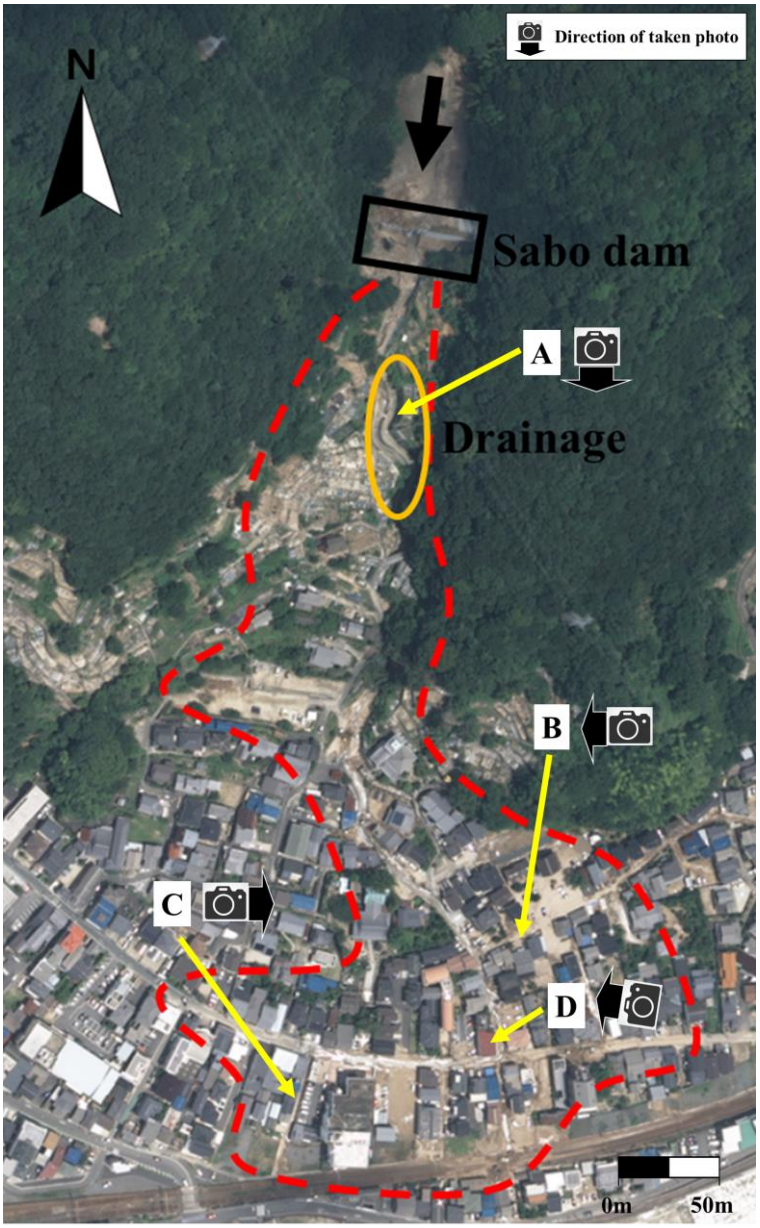

Fig. 3-2. Aerial photograph of Kaitacho, Aki-gun

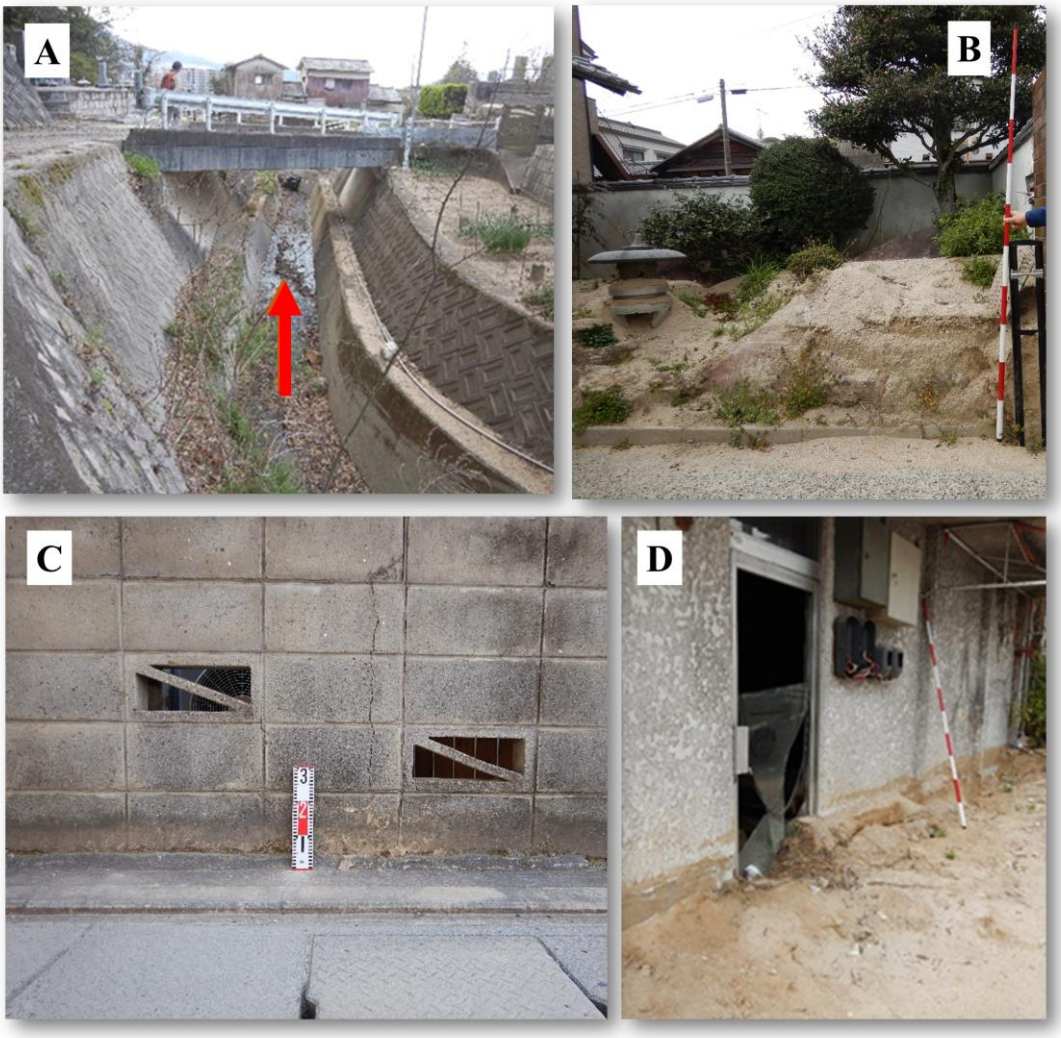

Fig. 3-3. Drainage and actual situation of damaged from SSF

3.2.1.2 Yanominami, Aki-Ku

Fig. 3-4 shows aerial photograph and actual situation of Yanominami, Aki-Ku. A sand pocket area (a width of 9m, a height of 4m and a length of 20m) was constructed right under sabo dam (Fig. 3-5). However, the outlet of drainage is narrow to pass the SSF to downstream. SSF moved to the left side after overflowed, because the right side is the upper slope area. SSF flowed along the roadway and some houses got damages like; damage to the wall, sediment inflows to houses and car was transferred. Because the roadway and houses located in right after the sand pocket area.

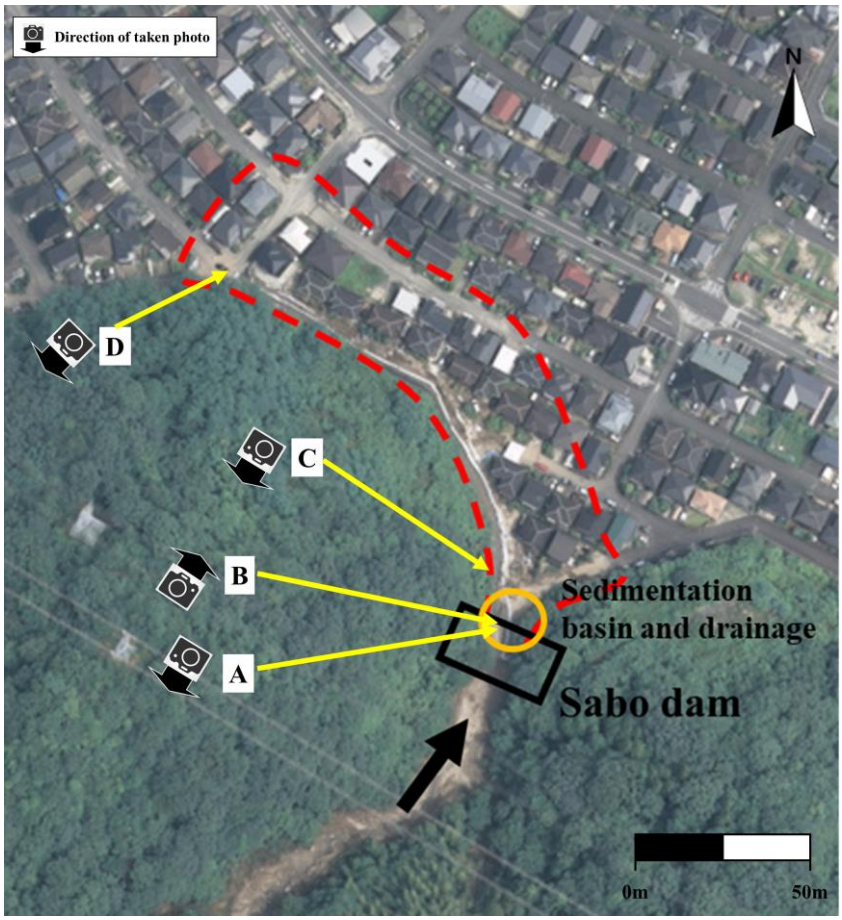

Fig. 3-4. Aerial photograph of Yanominami, Aki-Ku

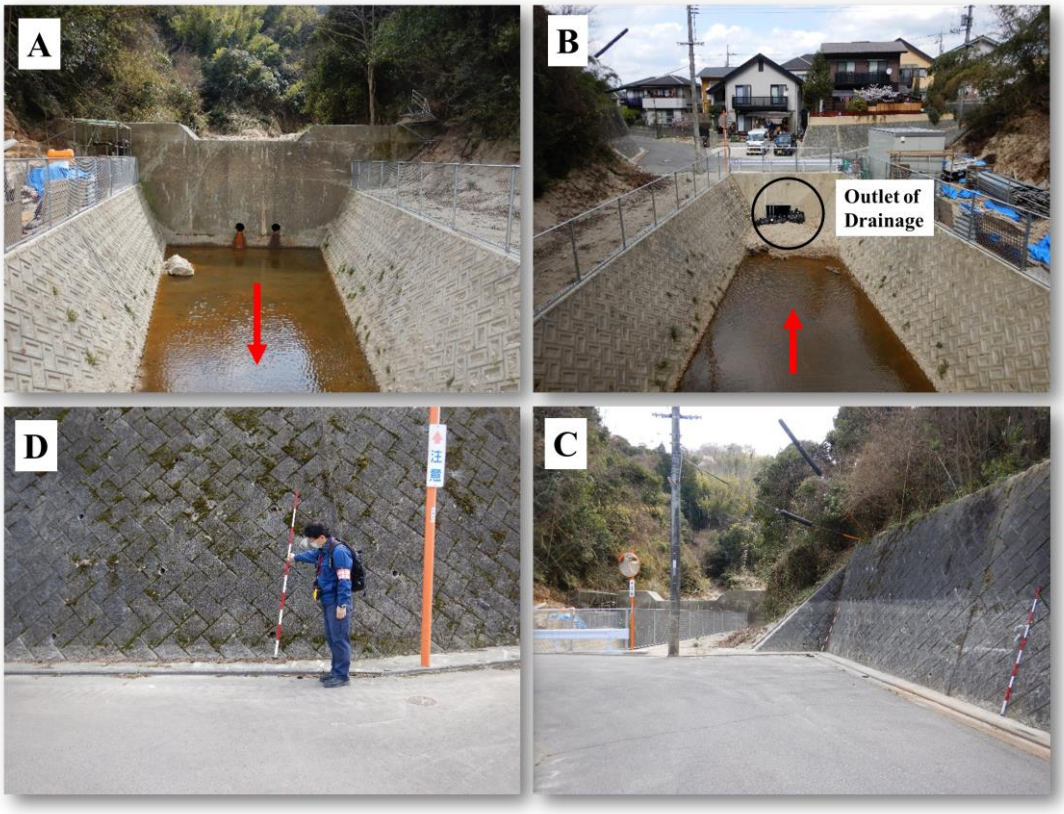

Fig. 3-5. Sediment retarding area and actual situation of damaged from SSF

3.2.1.3 Yanohigashi, Aki-Ku

Fig. 3-6 shows aerial photograph and actual situation of Yanohigashi, Aki-Ku. Survey area is a damaged area from debris flow of the No.1 (the red arrow) direction. In here, based on report [*Hiroshima prefecture*, 2018], the brown dotted line is damaged by debris flow. Houses collapsed or were swept away, and the deaths were also reported. There was a drainage, but the allowable discharge was small to prevent the damage. And the No.2 direction also occurred debris flow. Debris flow of No.1 and No.2 joined at the blue dot, and flowed downstream (Fig. 3-7).

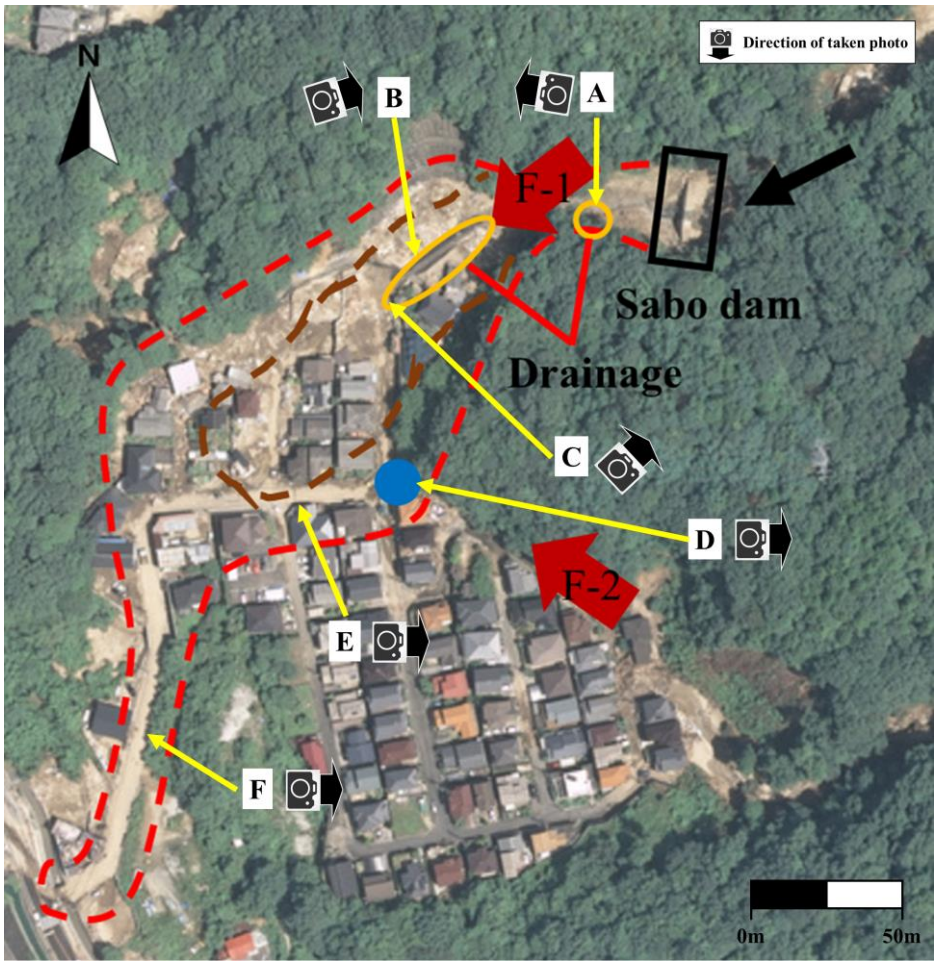

Fig. 3-6. Aerial photograph of Yanohigashi, Aki-Ku

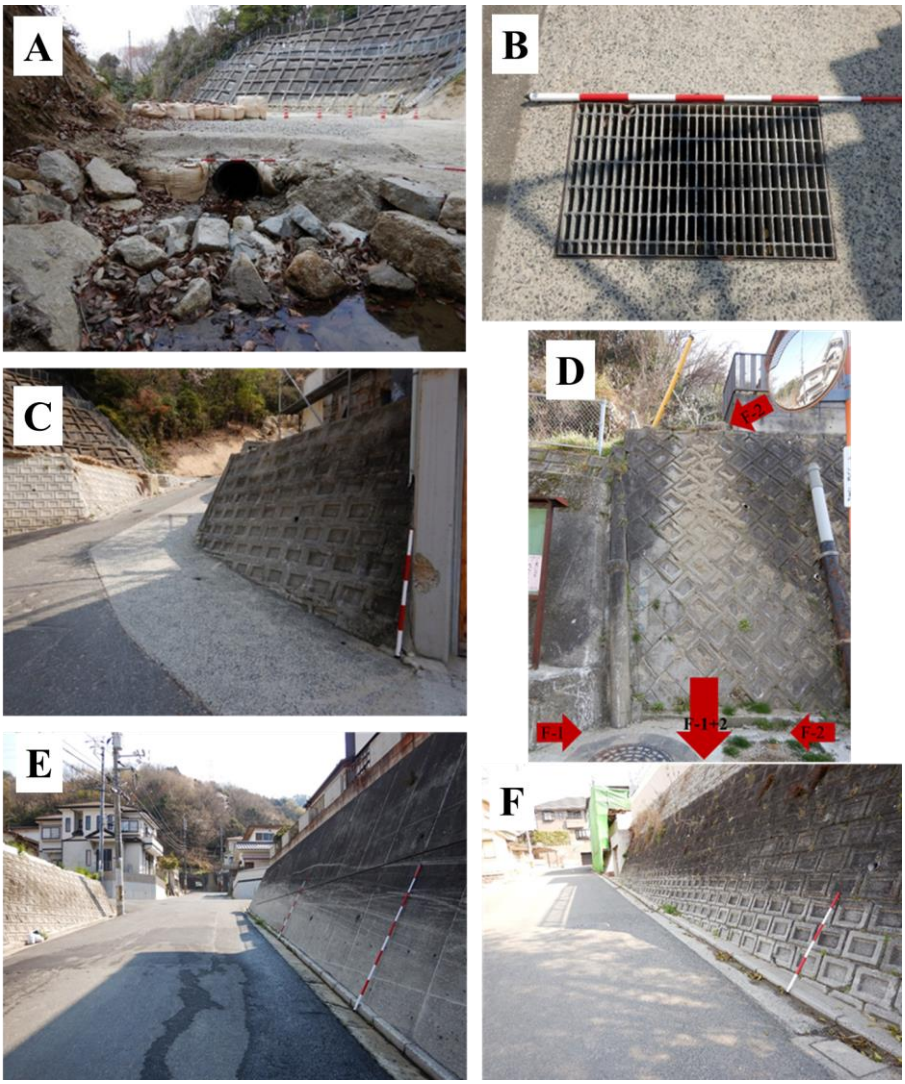

Fig. 3-7. Trace of debris flow and drainage

3.2.1.4 Tennodenjubaracho, Kure-Si

Fig. 3-8 shows aerial photograph and actual situation of Tennodenjubaracho, Kure-Si. The gradient is very steep where sabo dam is located, so the stepped drainage was constructed right under the sabo dam. And there are drainage and roadway under the tunnel. After passing throughout the tunnel, SSF moved to the center and left side, because the right side is the upper slope area. SSF flowed along the roadway, with curves, the traces of sedimentation were checked (Fig. 3-9).

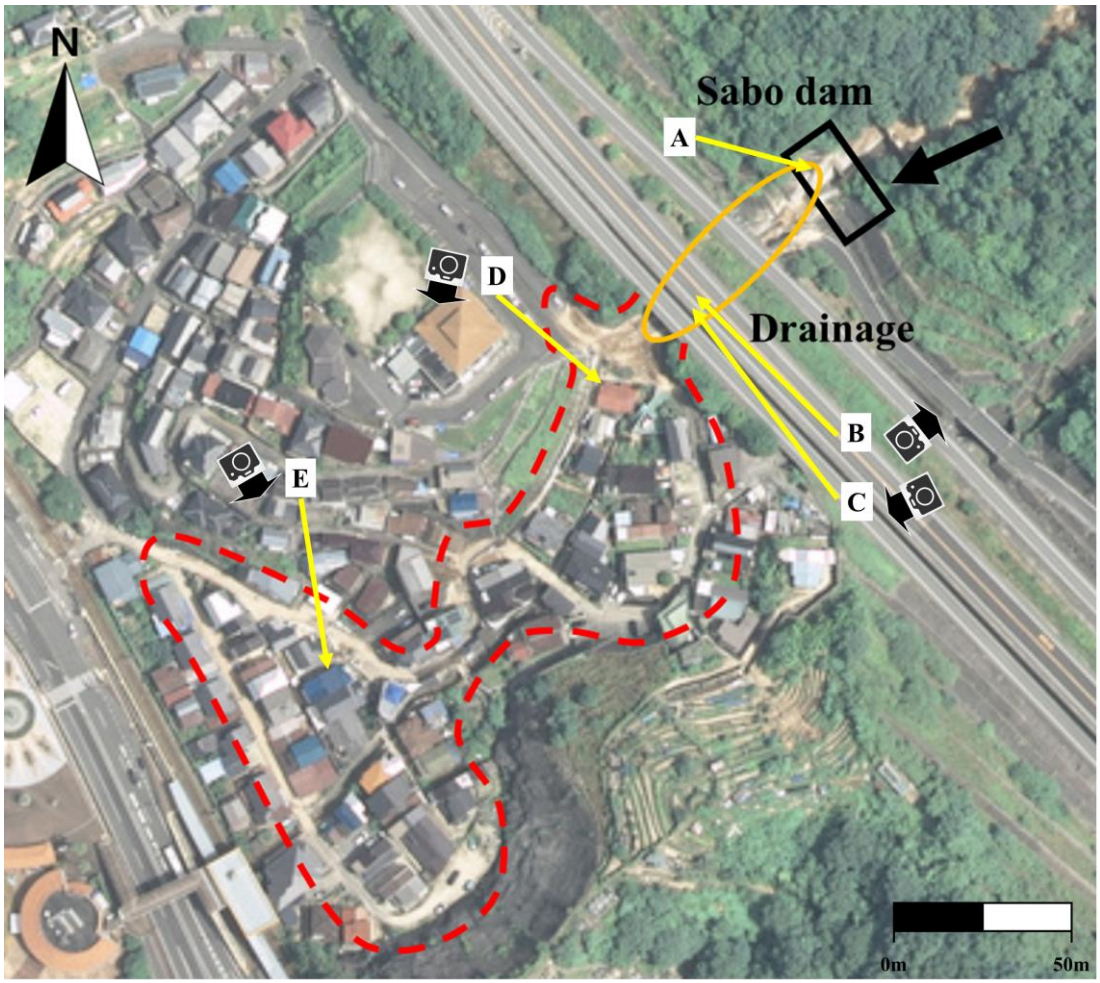

Fig. 3-8. Aerial photograph of Tennodenjubaracho, Kure-Si

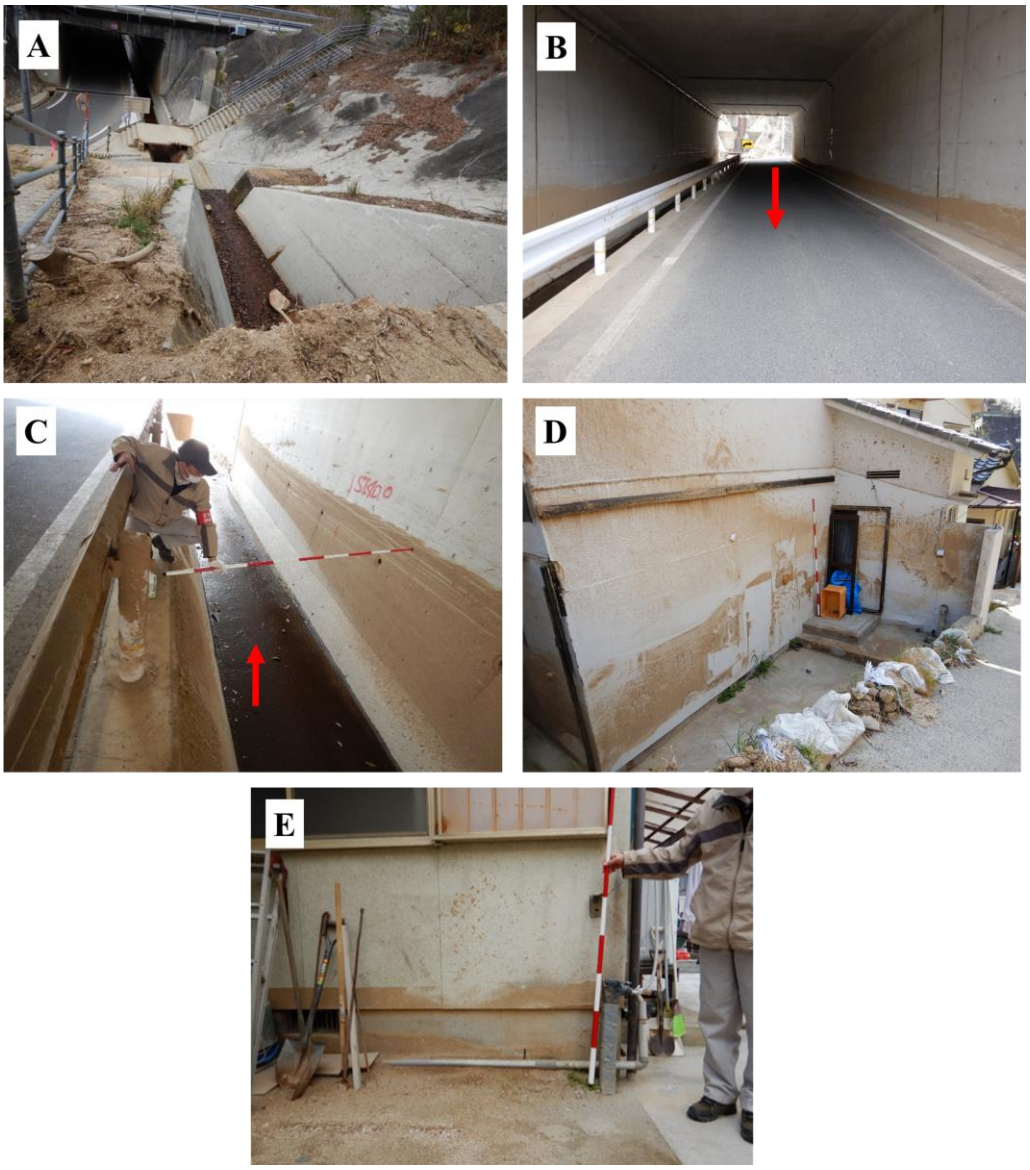

Fig. 3-9. Drainage and trace of SSF

3.2.2 Measurement

In order to confirm the discharge of the SSF, height of the SSF trace was measured by using ranging pole (Fig. 3-10). Also width and gradient were measured by laser range finder (Tru-pulse 200). Likewise, scale of drainage measured as same way (Fig. 3-11). Because for explaining the relationship between control capability of SSF and discharge of SSF in drainage.

Discharge of SSF was calculated by following formula;

$$Q = A \cdot V \quad (1)$$

Where, *Q*: discharge, *A*: cross-sectional area of flow, and *V*: velocity. Velocity can be calculated by the manning equation;

$$V = \frac{1}{n} \cdot R^{\frac{2}{3}} \cdot I^{\frac{1}{2}} \quad (2)$$

Where, *V*: mean velocity, n: coefficient of surface roughness (0.03), R: flow depth, and I: gradient of the survey point.

And, generally degree of damage is related with the hydrodynamic force. To calculate the hydrodynamic force of SSF, the density of flow is needed. However, this survey was conducted along the traces of SSF, so hydrodynamic force can be calculate with volume concentration. Volume concentration can be calculated by the following equation [*Mizuyama*, 1980];

$$\frac{qs}{q} = 5.5(tan\,\theta)^2 \quad (2)$$

Where, *q*: discharge, *s*: Volume concentration, and θ: gradient.

And then, weight per unit volume of SSF should be calculated. It can be calculated by the following equation;

$$\gamma_d = \{\sigma \cdot C_d + \rho \cdot (1 - C_d)\}g \quad (2)$$

Where, γ_d: weight per unit volume, σ: sediment density, C_d: concentration (volume concentration in this chapter), ρ: water density, and g: gravitational acceleration (9.8 m/s^2).

With values calculated so far, hydrodynamic force can be calculated by the following equation;

$$F = K_h \cdot \frac{\gamma_d}{g} \cdot D_d \cdot U^2 \quad (5)$$

Where, F : hydrodynamic force, K_h: coefficient (1.0), D_d: flow depth, and U: velocity.

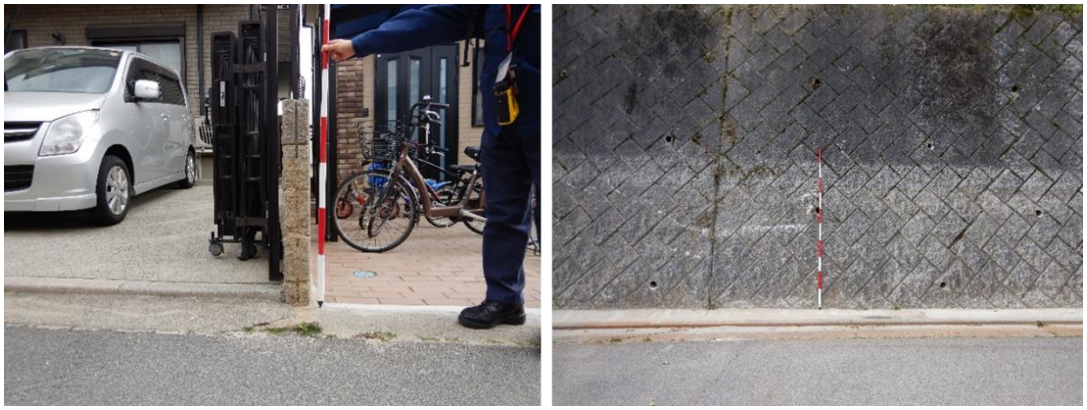

Fig. 3-10. Measuring a height of SSF trace by using ranging pole

Fig. 3-11. Measuring a scale of drainage

3.3 Result

Discharge of SSF, hydrodynamic force and scale of drainage were confirmed through field survey. The survey point was marked on the each figures and Table 3-1 shows the each result values. Cross sectional drawings and maps are from Geospatial Information Authority of Japan.

3.3.1 Kaita cho, Aki Gun

Flooded area, cross-section, and survey points, of Kaita Cho, Aki Gun, are shown in Fig.3-12. Discharge of No.1 was calculated separately due to the gradient and trace of SSF depth are different. In this area, the discharge of the SSF is 149.0 m^3/s (1(a) : 71.54 m^3/s, 1(b) : 77.49 m^3/s). SSF traveled almost 580 m along the roadway. The farther away from sabo dam, flow depth was getting lower (No.2 : 1.0 m ~ No.5 : 0.6m). Also the velocity was decreased as a lower gradient (No.2 : 6.0°, 8.3 m/s ~ No.5 : 1.0°, 2.6 m/s). And sediment deposit in the house and broken window was confirmed at No.5. SSF was spread to until A (flow depth : 0.3 m ~ 0.6 m) and B (flow depth : 0.2 m ~ 0.3 m) region. The hydrodynamic force was calculated as 309.3 kN/m (a) and 151.1 kN/m (b) in No.1. And it was decreased as farther (No.2 : 127.4 kN/m, No.5 : 5.9 kN/m).

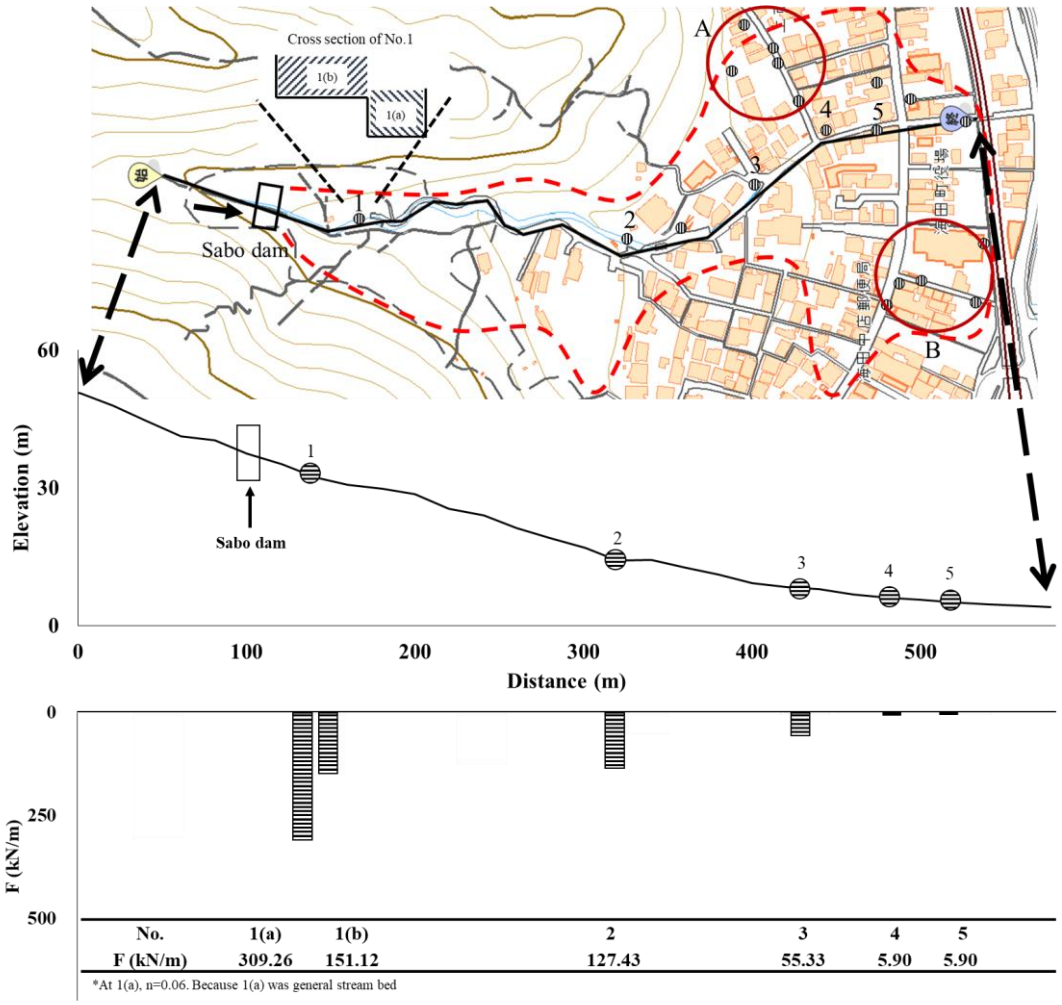

Fig. 3-12. Characteristics of damage (Kaita Cho, Aki Gun)

3.3.2 Yanominami, Aki-Ku

Flooded area, cross-section, and survey points, of Yanominami, Aki-Ku, are shown in Fig.3-13. Discharge of No.1 was 435.8 m^3/s. It is the largest value in the field survey because the cross-section area as large as 36 m^2. SSF flowed along the roadway from No.2, therefore discharge of SSF was decreased rapidly as decreased the cross-sectional area (from 435.8 m^3/s to 108.9 m^3/s). And discharge of SSF was decreased from 50.6 m^3/s to 3.6 m^3/s at No.3 and No. 7. The hydrodynamic force was calculated as 300.1 kN/m in No.1. And it was decreased as farther (No.2 : 175.2 kN/m, No.7 : 1.9 kN/m).

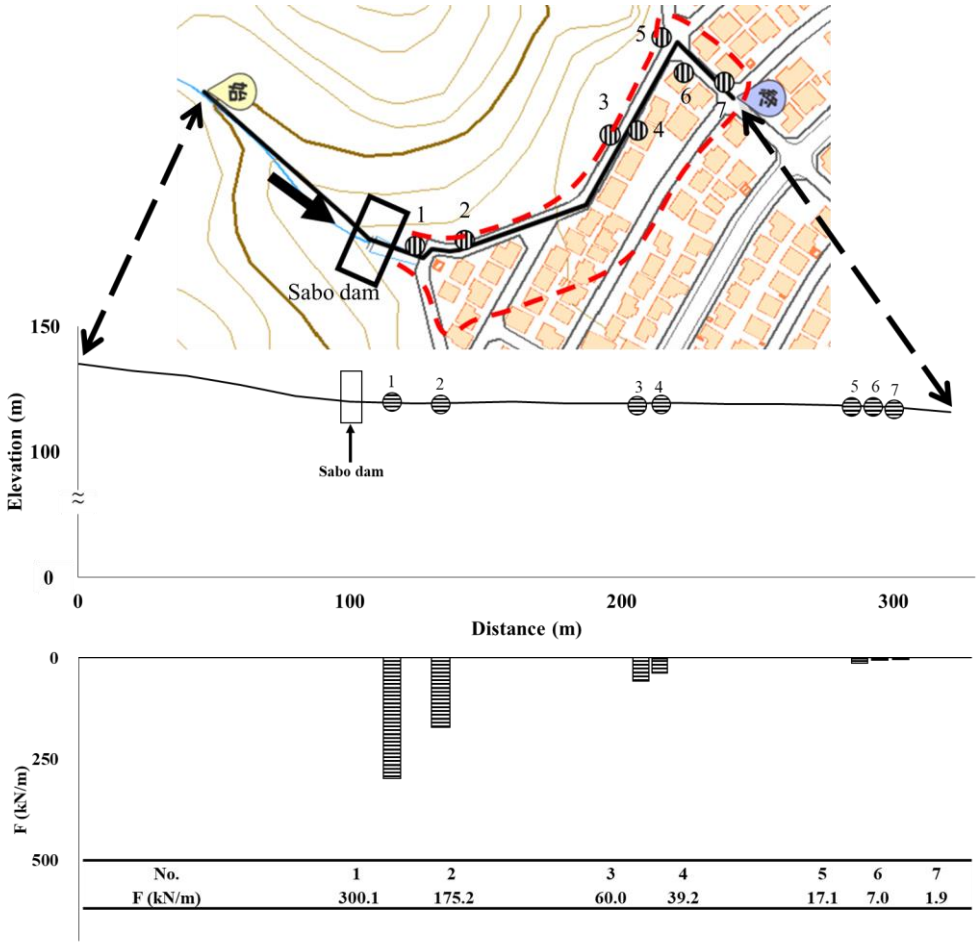

Fig. 3-13. Characteristics of damage (Yanominami, Aki-Ku)

3.3.3 Yanohigashi, Aki-Ku

Flooded area, cross-section, and survey points, of Yanohigashi, Aki-Ku, are shown in Fig.3-14. We surveyed the area that flow direction from L, and the area of brown dotted line was damaged by debris flow. So the survey was conducted No.1 to 3. Debris flow occurred also from the direction of R, and both SSF of L and R direction was combined. The flow depth of other survey areas was decreased as flow downstream, but the flow depth of No.1 ~ No.3 (0.9 ~ 1.0 m) was almost the same in this area. It seems that the SSF of R direction affected to No.3's flow depth. The hydrodynamic force was calculated as 91.9 kN/m in No.1 and 71.9 kN/m in No.2. The largest value was calculated in No.3 as 127.4 kN/m.

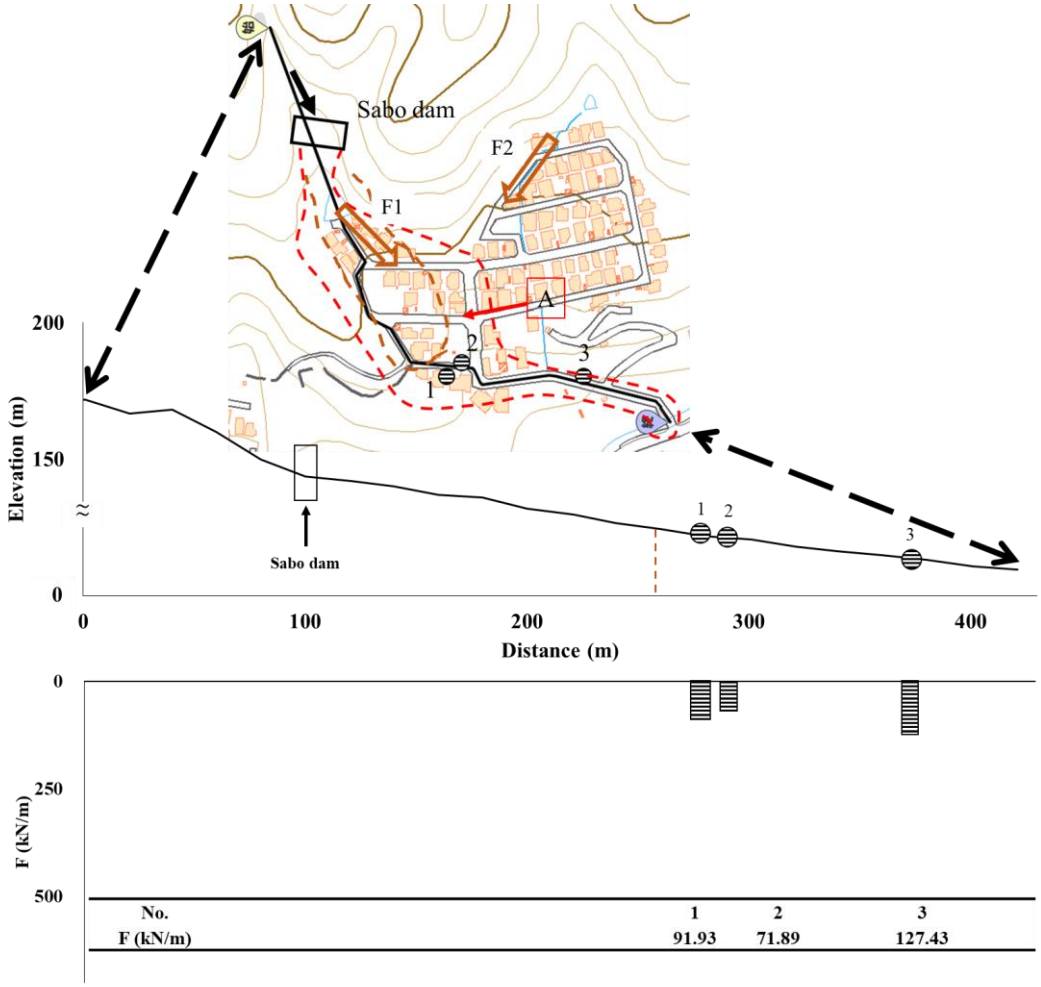

Fig. 3-14. Characteristics of damage (Yanohigashi, Aki-Ku)

3.3.4 Tennodenjubaracho, Kure-Si

Flooded area, cross-section, and survey points, of Tennodenjubaracho, Kure-Si, are shown in Fig.3-15. This area has less discharge of SSF than other areas. No.1 is a tunnel with a drainage (1(a)) and a roadway (1(b)), value of discharge was 62.1 m^3/s and 17.1 m^3/s. From No.3 to No.8, the flow depth was low as 0.6 m ~ 0.2 m but the slope was 7° ~ 9.5°, so the discharge of SSF was small but it flowed as high velocity. The hydrodynamic force was calculated the largest value as 677.8 kN/m at 1(a) because the velocity was high due to a steep concrete drainage. Except for 1(a), discharge was large as 69.4 m^3/s at No.3 and the rest was calculated to be less than that.

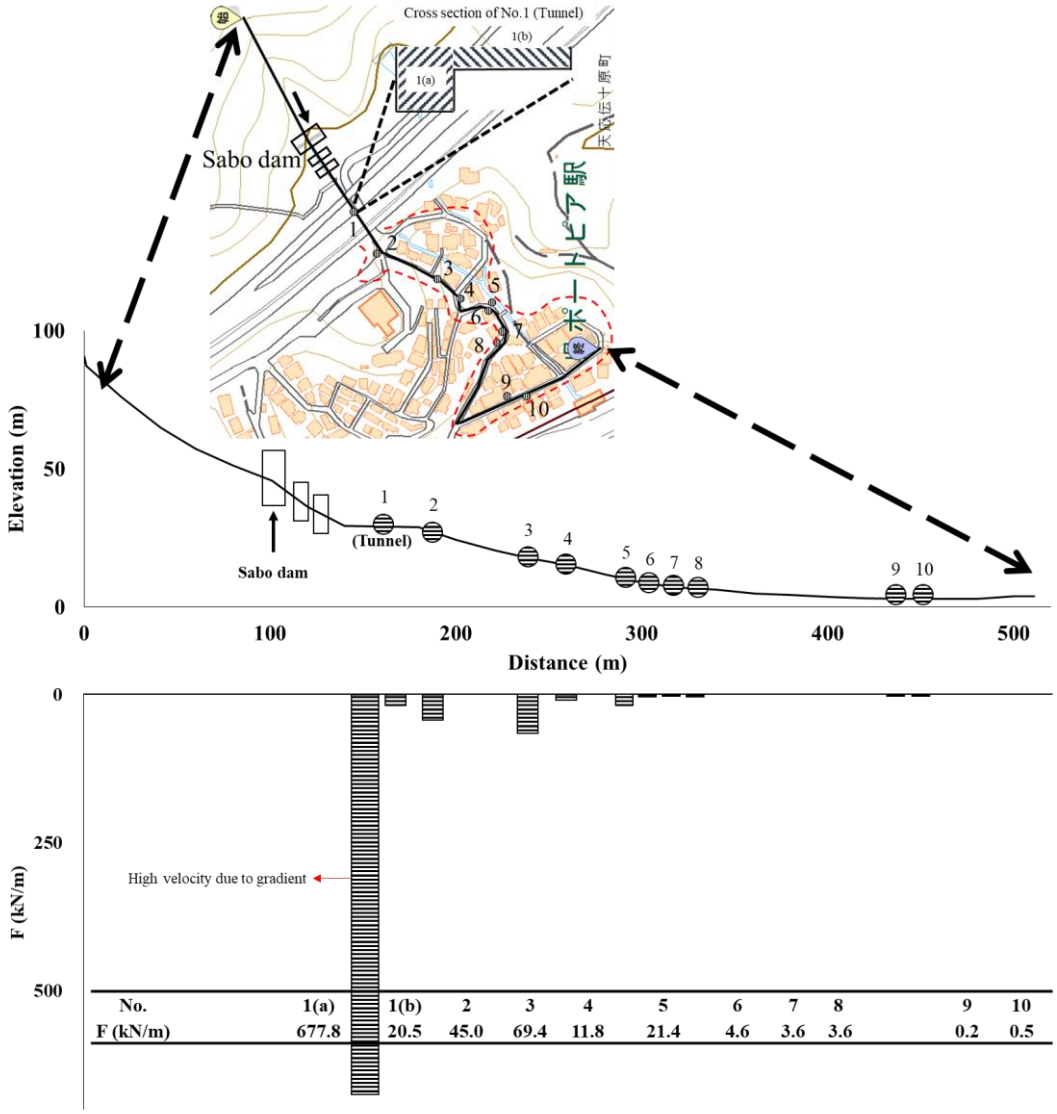

Fig. 3-15. Characteristics of damage (Tennodenjubaracho, Kure-Si)

Table 3-1. Measurement and calculation values in each survey site

Study site	No.	Flow depth (m)	Width (m)	Gradient (°)	Velocity (m/s)	Cross section area (m^2)	Discharge (m^3/s)		F (kN/m)
(a)	1(a)	2.2	3.0	8.5	10.8	6.6	71.54	149.0	309.3
	1(b)	1.8	5.0	7.0	8.6	9.0	77.49		151.1
	2	1.0	4.0	6.0	10.8	4.0	43.1		127.4
	3	0.9	4.0	4.0	7.9	3.4	26.9		55.3
	4	0.6	4.0	1.0	3.1	2.4	7.5		5.9
	5	0.6	6.0	1.0	3.1	3.6	11.3		5.9
(b)	1	2.0	18.0	3.0	12.1	36.0	435.8		300.1
	2	1.9	6.0	2.0	9.6	11.4	108.9		175.2
	3	1.2	6.0	2.0	7.0	7.2	50.6		60.0
	4	1.0	6.0	2.0	6.2	6.0	37.4		39.2
	5	0.7	6.0	2.0	4.9	4.2	20.6		17.1
	6	0.4	6.0	3.0	4.1	2.4	9.9		7.0
	7	0.2	6.0	4.0	3.0	1.2	3.6		1.9
(c)	2	1.0	5.0	4.5	9.3	5.0	46.7		91.9
	3	0.9	5.0	4.5	8.7	4.5	39.2		71.9
	4	1.0	6.5	6.0	10.8	6.5	70.1		127.4
(d)	1(a)	1.7	2.0	8.5	18.3	3.4	62.06	79.1	677.8
	1(b)	0.5	5.5	5.0	6.2	2.8	17.05		20.5
	2	0.7	7.0	5.0	7.8	4.9	38.0		45.0
	3	0.6	2.0	9.5	9.6	1.2	11.6		69.4
	4	0.3	4.0	8.5	5.7	1.2	6.9		11.8
	5	0.4	4.0	8.0	6.8	1.6	10.8		21.4
	6	0.2	4.0	8.5	4.4	0.8	3.5		4.6
	7	0.2	4.0	7.0	4.0	0.8	3.2		3.6
	8	0.2	4.0	7.0	4.0	0.8	3.2		3.6
	9	0.2	4.0	1.0	1.2	0.6	0.7		0.2
	10	0.2	4.0	1.0	1.5	0.8	1.2		0.5

3.3.5 Relationship between discharge of SSF and scale of drainage in each site

Sites of (a) to (d) correspond to Fig.3-1.

(a) The discharge of SSF was 149.0 m^3/s. The drainage was constructed on the left side of SD (direction of downstream), and the allowable discharge of drainage which can control the SSF was 62.0 m^3/s (42%).

(b) The discharge of SSF was 435.8 m^3/s. There was sediment retarding area right under the SD, but it was not enough to retard the SSF and the allowable discharge of drainage which can control the SSF was 10.8 m^3/s (2%). The value of discharge of SSF was large because the width was wide in this area.

(c) In this area, the debris flow flowed to the residential area, therefore, we couldn't measure the discharge of SSF. The allowable discharge of drainage which can control the SSF was just 1.0 m^3/s.

(d) The discharge of SSF was 79.1 m^3/s. The allowable discharge of drainage under the tunnel which can control the SSF was 34.9 m^3/s (44%), and the another drainage which located in residential area was 20.5 m^3/s (25%).

3.4 Conclusion

In order to confirm the necessity of study for effective SSF countermeasures to mitigate the SSF in high population density area, the field survey was conducted in damaged areas by SSF. The characteristics of the SSF occurred in Hiroshima in July 2018, and the allowable discharge of the drainages were also calculated. In addition, the land use was confirmed as to why SSF countermeasures were not constructed.

The actual situation of damages caused by SSF was mostly found as sediment inflows to houses, parking lots, and gardens, and where glass was broken. And in the case of the survey area (a), the range of the damage was checked up to 500 meters or more, so it was able to identify damage to extensive area by the SSF.

In the land use at each site,

(a) There is a cemetery right side of just downstream of the SD. The drainage was constructed on the left side, but the SSF spread widely. And many houses were located in downstream.

(b) The distance between SD and the roadway was only 20 m away. And there were houses right away.

(c) The high population density area was located about 70 m from the SD.

(d) There is roadway and drainage under the tunnel in the 10 m downstream from the SD. The roadway connected to downstream and also many houses were located there.

Yamada [2018] reported the relation with damage degree and hydrodynamic force; Degree 1. Lose (at least 150 kN/m), 2. Horizontal dislocation (at least 100 kN/m), 3. Be completely destroyed (at least 60 kN/m), 4. Be partially destroyed (at least 10 kN/m), 5.

Damage (at least 1 kN/m), 6. The slight sedimentation (under 1 kN/m). With the results of the field survey, 42% of survey points had hydrodynamic force enough to be completely destroyed the houses (including the survey points in the lower of SD which houses are not located)(Fig. 3-16). Although the house has not been destroyed due to SSF, care must be taken as there is a possibility.

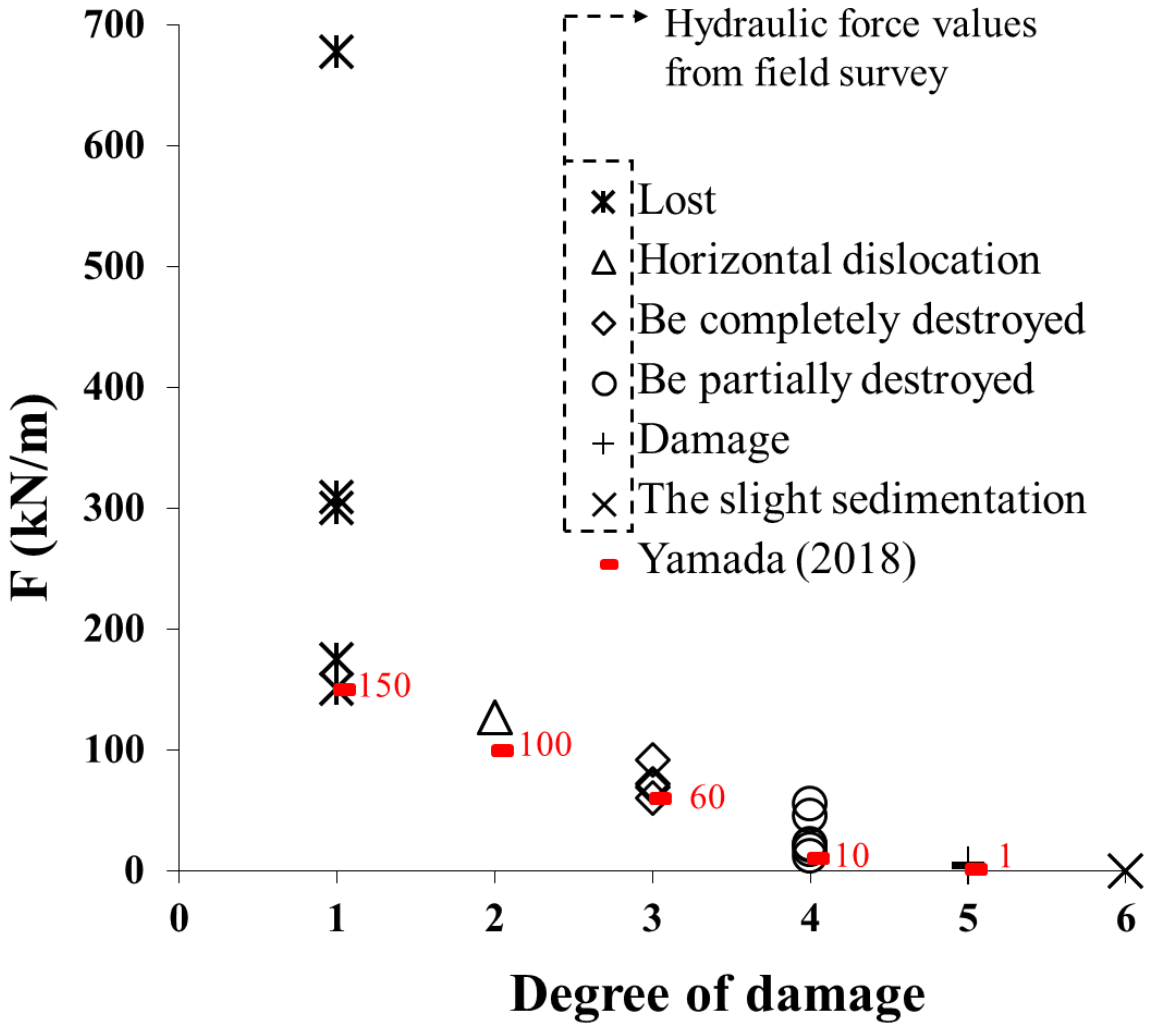

Fig. 3-16. The relation with damage degree and hydrodynamic force

For this reason, it seemed difficult to construct channel works or sediment retarding basin. Also all sites had insufficient allowable discharge of drainage to control the SSF. Of course, it seems impossible to remove houses and roadways in residential areas, and also construct channel works or sediment retarding basin without remove houses and roadways. This is why the other effective SSF countermeasures are necessary to mitigate the SSF as much as possible near the SD.

Chapter 4

Experimental study on physical measures against subsequent sediment flow

(SSF breaker, polymer, and sub-dam)

4.1 Introduction

As mentioned in Chapter 1, the flume experimental was conducted using experimental countermeasure structures (SD, SSF breaker, polymer, and sub–dam). The purpose of this experiment is reduction of hydrograph by reducing the outflow discharge and sediment concentration of SSF.

4.2 Method

In the flume experiment, we first trapped a simulated debris flow using a model sabo dam and then controlled SSF using models of an SSF breaker, water-absorbing polymer, and sub-dam. The experimental conditions are shown in Fig.4-1. The experimental flume comprised an upper part (140 cm long, 6.5 cm wide, 10 cm high, 18° gradient) and a lower part (25 cm long, 7.8 cm wide, 10 cm high, 10° gradient). To generate a debris flow, we fixed debris (625 cm^3, d_{50} = 1.5 mm) at the upper part of the flume and provided a constant supply of water (250 cm^3/s) from upstream of the debris for 2.5 s. The amount of supplied debris was determined according to the sediment volume in a sabo dam at full deposition. The full depositional gradient was set at $1/2\theta_u$ following a preliminary experiment, where θ_u is the gradient of the upper part of the flume. Water was supplied for a final debris flow concentration of approximately 40%, with a sediment:water ratio of 1:1.

One sabo dam model was installed at the gradient inflection point (equivalent to a valley exit) to capture debris. An SSF breaker model (length, 15 cm) was attached to the sabo dam model to induce sedimentation of SSF. The SSF generation process is

shown in Fig.4-2. We collected SSF samples at the outlet at the bottom part of flume; these samples were used to estimate particle diameter (mean: 0.7 mm, d_{90}: 3 mm, d_{max}: 4 mm). We therefore varied the opening size of the breaker, setting it at 0, 0.5, 0.7, 1, 2, 3, 3.5, and 4 mm to determine the optimal breaker opening size (Fig.4-3).

We selected CP-1 as the water-absorbent polymer and performed an absorption ability test (AAT) to determine the suitable amount of polymer for the experiment (Fig.4-4). The AAT was conducted under the static condition using 600 mL SSF and 150, 300, 450, and 600 mL water (i.e., ratios of 1/4, 1/2, 3/4, and 1). The initial amount of polymer was 1.2 g, which is able to absorb up to 600 mL of water (about 300–500 times its mass); the polymer mass was set at 1.2, 3, 5, 10, 20, 30, 40, 50, and 60 g. The time elapsed until gelation was calculated by adding *t0* and *t1* (*t0*: the moment of water contact with polymer, *t1*: the moment of finishing the gelation).

A sub-dam model was installed in the flume to trap sediment and create a pool to increase absorption by the polymer. To determine the location and height of the sub-dam, we considered the effects of compaction. The sub-dam was placed at the point of sediment outflow from the SSF breaker, i.e., 12 cm downstream from the sabo dam. A sub-dam with a height of 5.8 cm was found to trap the entire SSF. We therefore conducted experiments using four sub-dam heights: 2.2, 3.5, 4.6, and 5.8 cm (i.e., 1/4, 1/2, 3/4, and 1 of the total height).

Therefore, we performed a total of 18 experiments (Cases 1–18) with varying parameters (Table 4-1). Case 1 was designed to determine the fundamental SSF conditions of the sabo dam model. In Cases 2–9, we added the SSF breaker model, varying the breaker opening size. The peak discharge, elapsed time, and SSF

concentration results of Cases 2–9 allowed us to determine the effective SSF breaker opening size (2 mm, Case 6). In case 10, we added the water-absorbent polymer. In Cases 11–14, we added the sub-dam model to Case 6. Cases 15–18 were conducted using all three experimental countermeasure structures. We measured the time elapsed from the sabo dam to the end of the flume, sediment volume at the SSF breaker, peak discharge, and concentration in all experiments to determine the effectiveness of the experimental countermeasure structures. All experiments were videotaped in side view. SSF samples were collected using a catchment box at an outlet at the bottom part of the flume to calculate sediment volume and weight; a hydrograph and SSF concentration was analyzed by using 10 samples. Concentration was calculated from the total SSF volume and sediment volume. SSF peak discharge was determined using the hydrograph, where peak discharge was the highest value.

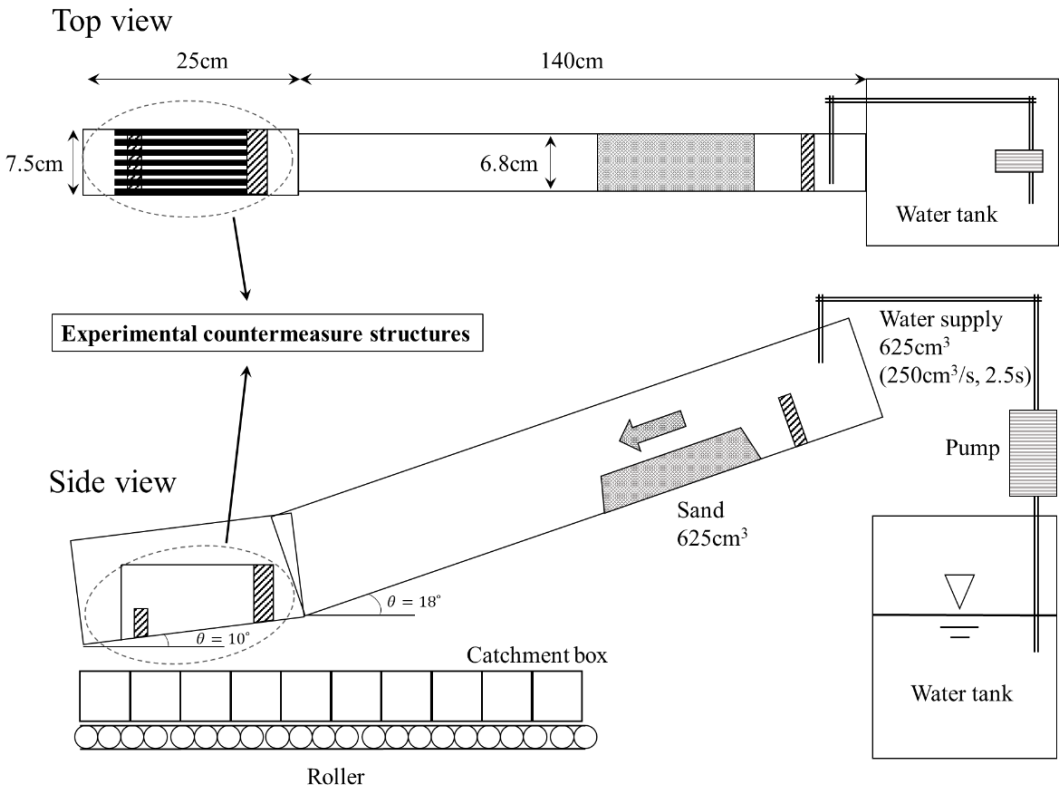

Fig. 4-1. Sketch of experimental flume

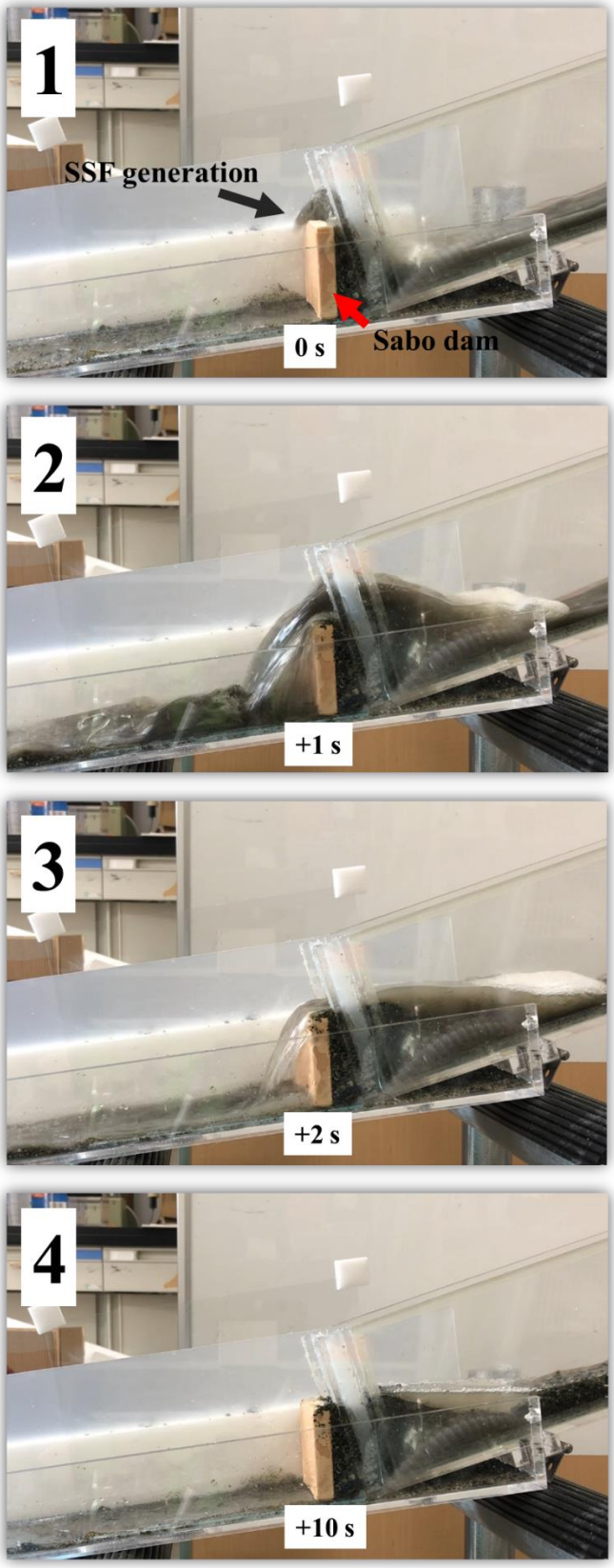

Fig. 4-2. Process of SSF in this study

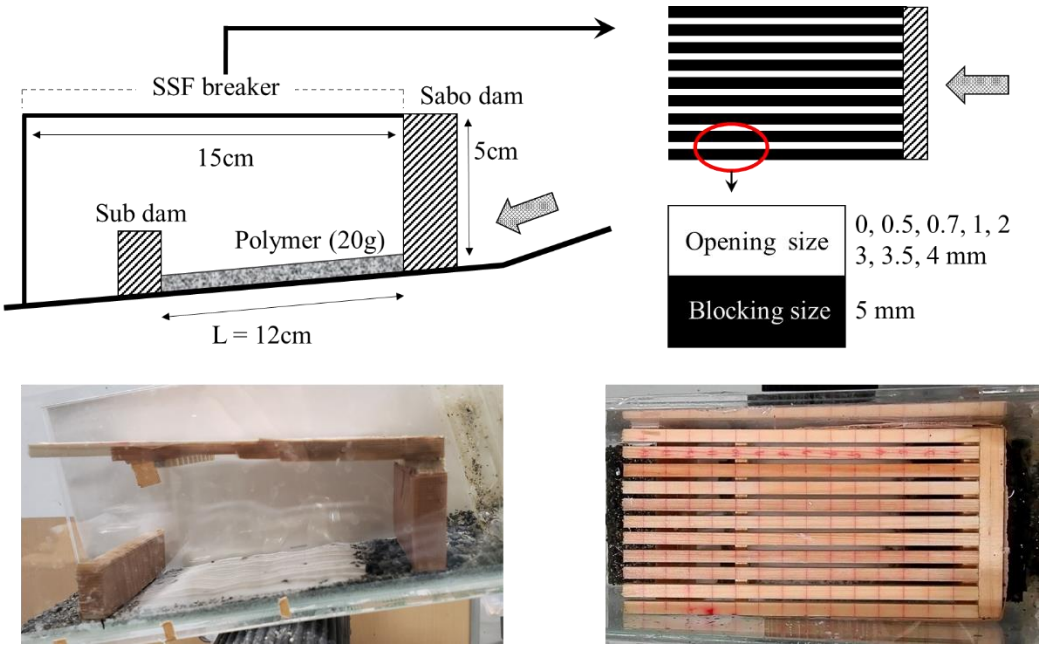

Fig. 4-3. Composition of experimental countermeasure structures

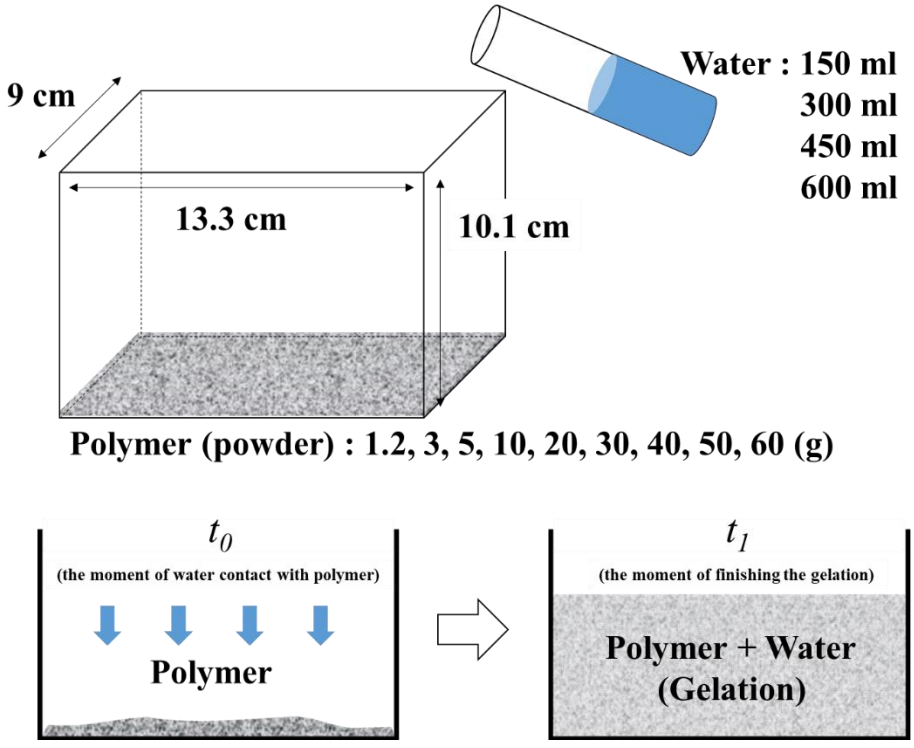

Fig. 4-4. Process of the Absorption Ability Test (AAT)

4.3 Result

4.3.1 Polymer absorption ability

The AAT results showed that the optimal amount of polymer was 20 g (Fig.4-5); even if larger amounts of polymer supplied to water, resulted in gelation within approximately the same amount of time.

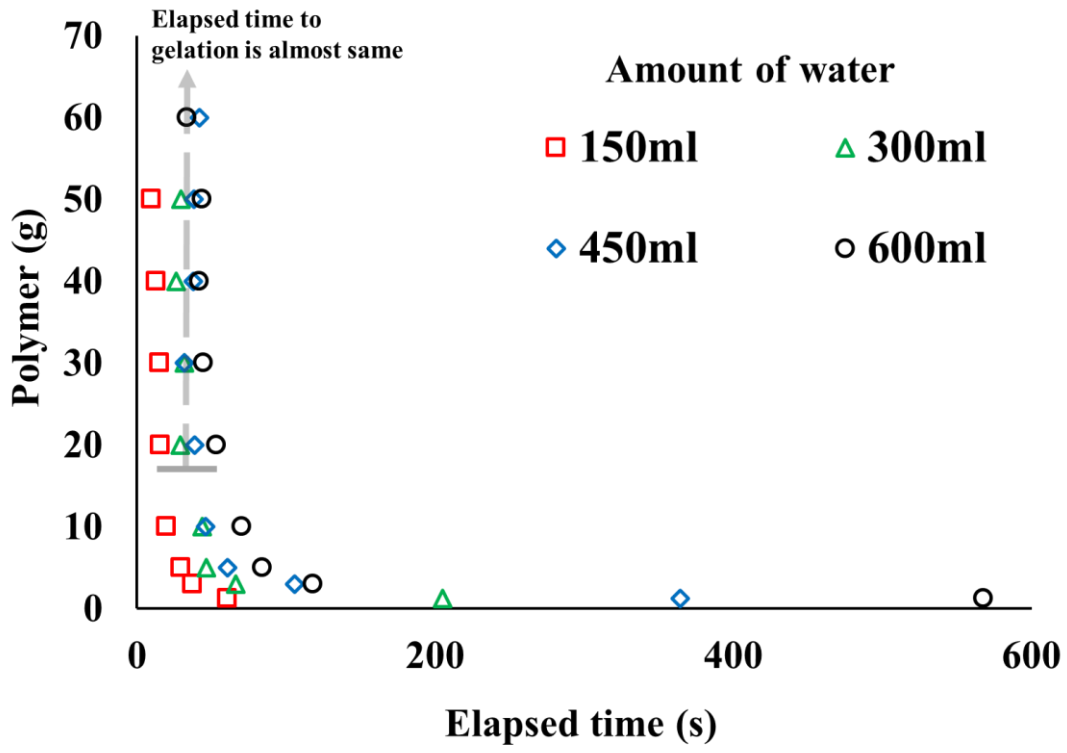

Fig. 4-5. Result of Absorption Ability Test (AAT)

Table 4-1. Experimental cases and result values of each case

	Case	L_s(cm)	S_i(mm)	$d_{50(s)}/S_i$	Sub-dam$_h$(cm)	Elapsed time(s)	V_s(cm^3)	C(%)	Q_p(cm^3/s)
SD	Case1					0.72		14.34	337.65
SD + SSF breaker	Case2	15	0.00			0.56	15.02	5.97	195.19
	Case3		0.50	2.13		0.79	14.05	3.84	154.59
	Case4		0.70	1.53		0.77	12.12	3.43	147.80
	Case5		1.00	1.08		0.84	11.31	2.97	132.22
	Case6		2.00	0.54		0.86	9.53	3.19	131.89
	Case7		3.00	0.36		0.85	4.85	8.66	136.37
	Case8		3.50	0.33		0.76	2.91	11.80	150.62
	Case9		4.00	0.29		0.77	2.26	12.61	146.98
SD + SSF breaker + P(20)	Case10		2.00	0.54		0.82	9.21	2.51	135.21
SD + SSF breaker + Sub-dam	Case11				2.20	1.52	10.18	1.08	63.63
	Case12				3.50	3.61	8.24	0.08	30.82
	Case13				4.60	4.85	10.02	0.00	26.35
	Case14				5.80		8.88	0.00	0.00
SD + SSF breaker + P(20) + Sub-dam	Case15				2.20	1.44	9.37	0.43	60.64
	Case16				3.50	2.76	10.66	0.05	41.26
	Case17				4.60	5.13	11.15	0.00	22.37
	Case18				5.80		10.98	0.00	0.00

*SD : Sabo dam, P(20) : Polymer 20g, L_s : Length of SSF breaker, $d_{50(s)}$: mean particle size of sediment on SSF breaker, S_i : Interval of SSF breaker, Sub-dam$_h$: Height of Sub-dam, V_s : Volume of sediment on the SSF breaker, Q_p : Peak discharge

4.3.2 SSF breaker performance

Examples of the SSF breaker performance in Cases 2–9 are shown in Fig.4-6. The breaker effectively reduced elapsed time, peak discharge, and SSF concentration (Fig.4-7). The longest elapsed time was observed in Case 6 (0.86 s), which took 0.14 s longer than Case 1. The highest peak discharge was observed in Case 1 (337.7 cm^3/s), followed by Case 2 (195.2 cm^3/s, a 42.2% decrease). The smallest peak discharge was observed in Case 6 (131.9 cm^3/s), which was 61.9% lower than that in Case 1. The largest sediment volume at the SSF breaker was observed in Case 2 (15 cm^3), and the smallest in Case 9 (2.3 cm^3). The breaker opening size affected both elapsed time and peak discharge; narrower openings led to sediment overflow, and large amounts of sediment passed through the breaker when openings were wider. In Case 1, SSF concentration was 14.34%, whereas that in Case 9 was 12.61%, representing a 12.1% decrease. The lowest SSF concentration was observed in Case 5 (2.97%), which was 79.3% lower than that in Case 1. Among all cases, Case 6 showed an elapsed time of 0.86 s, peak discharge of 131.9 cm^3/s, and concentration of 3.19%, demonstrating optimal effectiveness among the experimental cases. Therefore, subsequent experiments were performed using a breaker opening size of 2 mm.

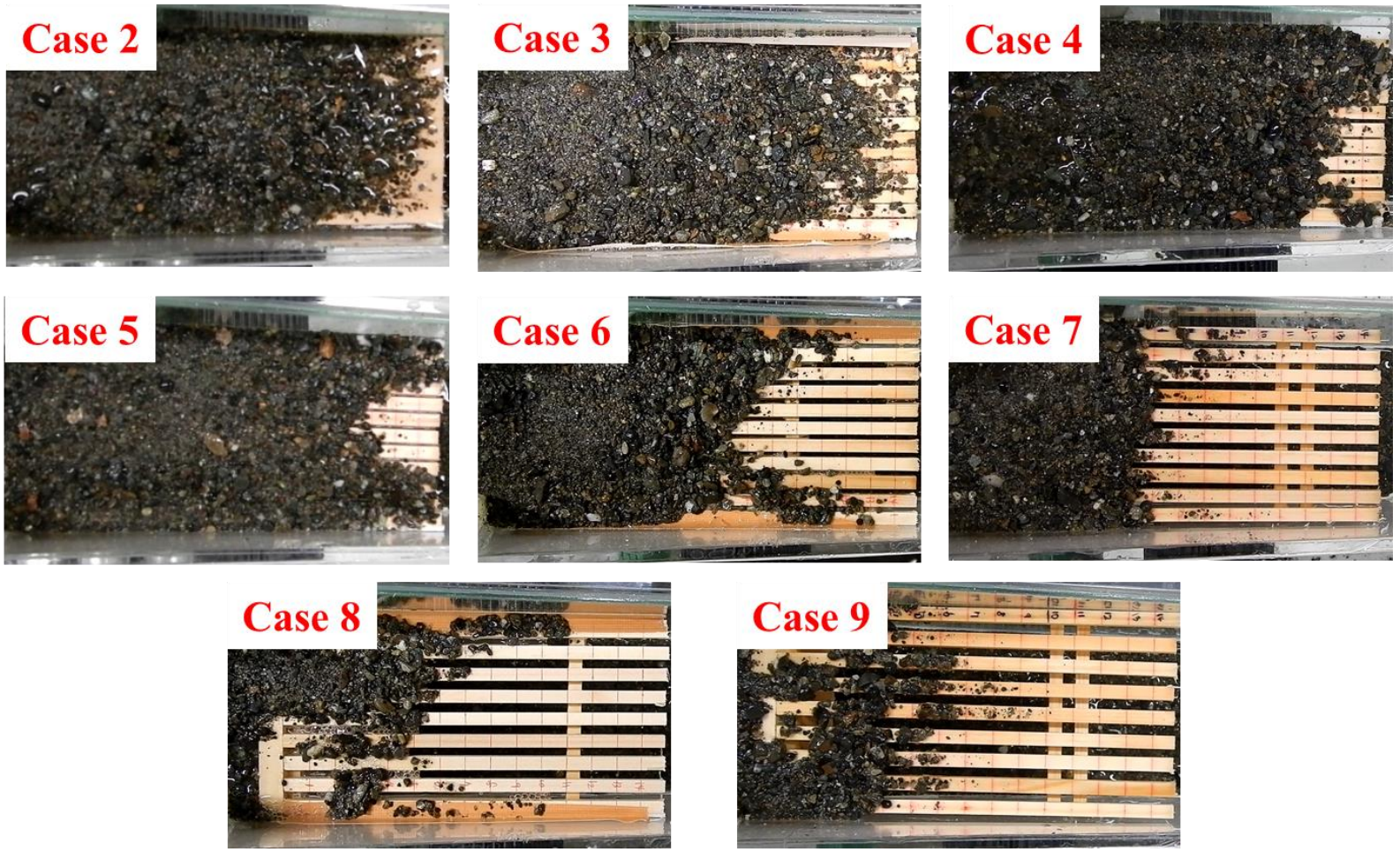

Fig. 4-6. Result of deposition on the SSF breaker (case 2 to 9)

4.3.3 Combined application of both SSF breaker and polymer

In Case 10, we recreated the Case 6 conditions and added the water-absorbing polymer. The result was an elapsed time of 0.82 s, peak discharge of 135.2 cm^3/s, SSF breaker sediment volume of 9.2 cm^3, and concentration of 2.51%. These values are nearly the same as those obtained in Case 6, demonstrating that polymer application had no significant effect on the measured parameters.

4.3.4 Combined application of both SSF breaker and sub-dam

In Cases 11–14, we applied both the SSF breaker and sub-dam; hydrographs for these experiments are shown in Fig.4-8. The addition of the sub-dam clearly increased the elapsed time and decreased the concentration and peak discharge. Compared with Case 1, the elapsed time increased by 0.8 to 4.13 s, depending on the height of the sub-dam. Peak discharge was reduced by more than 81%. Sediment was deposited at the sub-dam, decreasing the concentration by 92%. In Case 13, all of the sediment was deposited, and only water continued to flow downstream. As the sub-dam height increased, SSF mitigation was more effective, and the polymer gelation period increased. In Case 14, we could not measure elapsed time, peak discharge, or concentration because all sediment was deposited at the sub-dam, preventing further SSF.

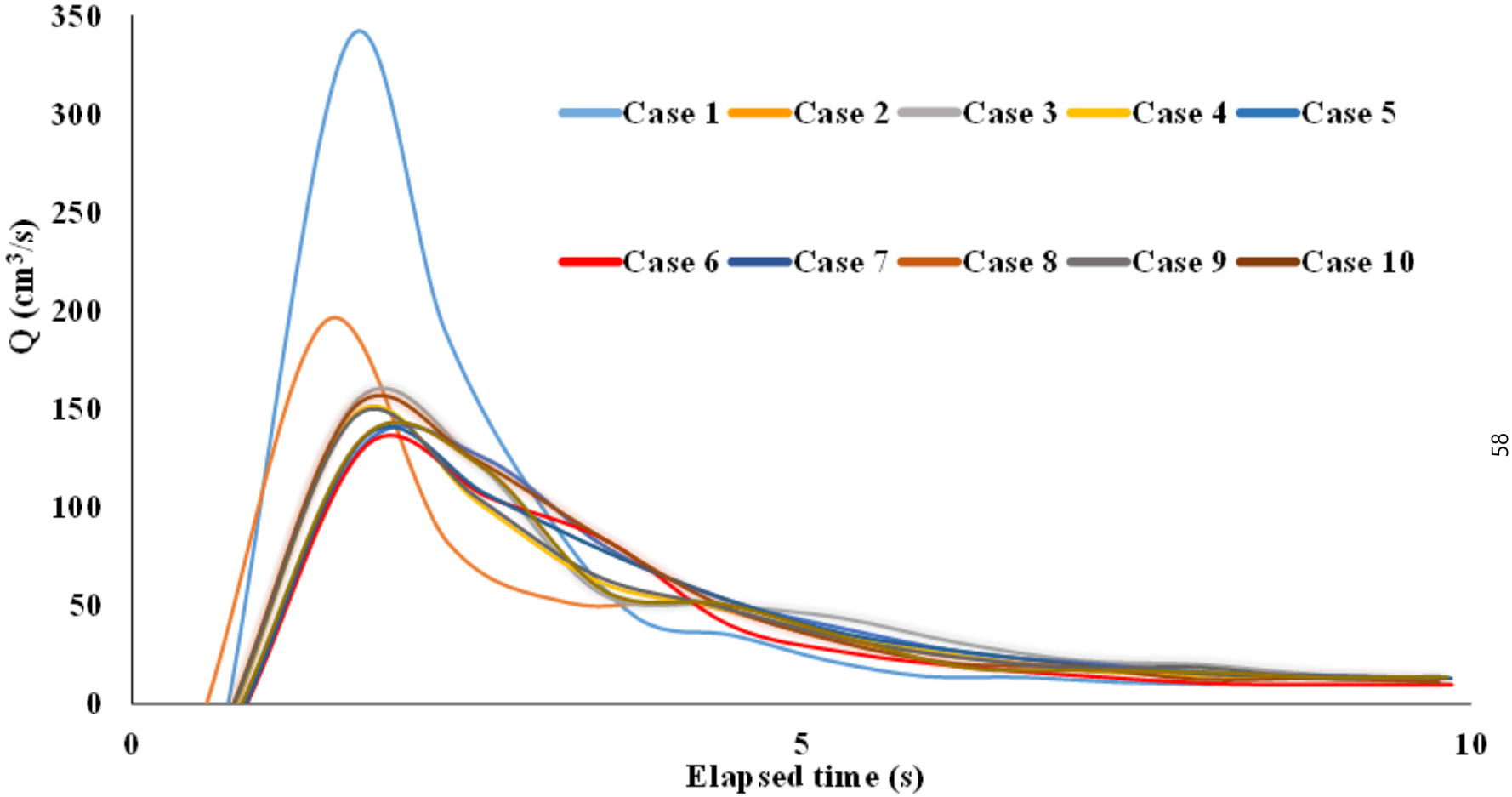

Fig. 4-7. Hydrograph of SSF (SD only, SD and SSF breaker)

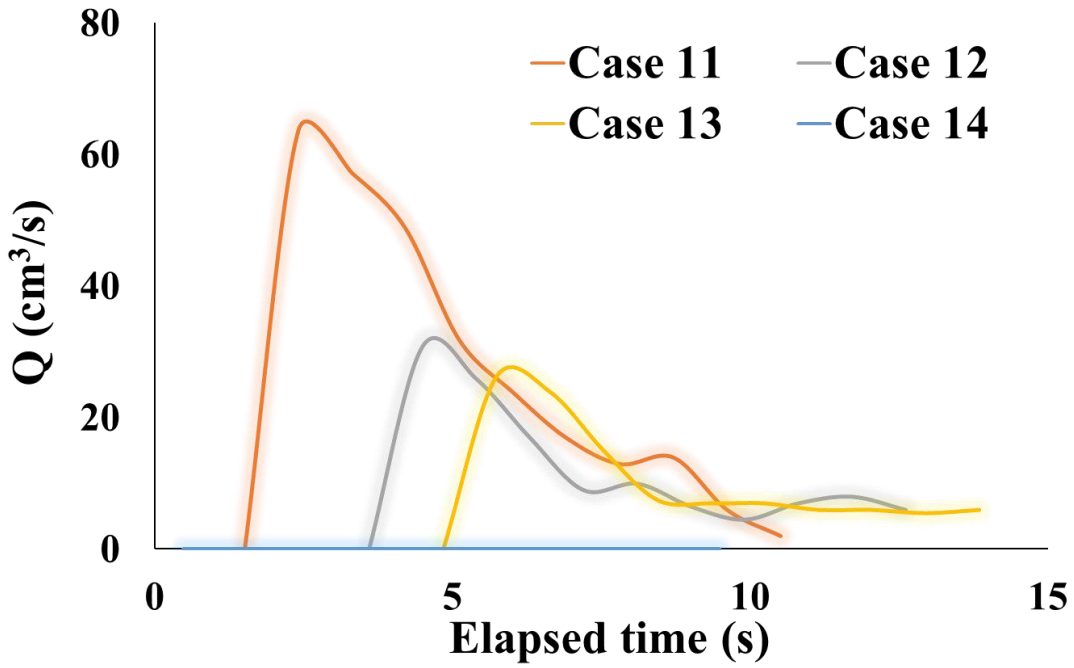

Fig. 4-8. Hydrograph of SSF (SD, SSF breaker and Sub-dam)

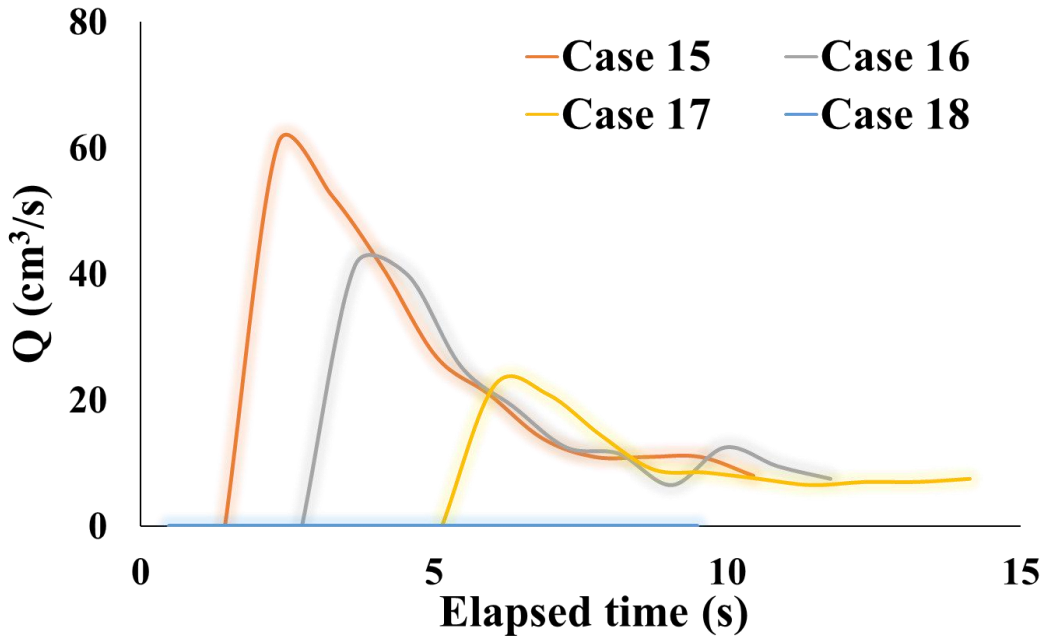

Fig. 4-9. Hydrograph of SSF (SD, SSF breaker, Sub-dam, and P(20))

4.3.5 Combined application of the SSF breaker, sub-dam, and polymer

In Cases 15–18, we installed the SSF breaker, sub-dam, and polymer downstream of the sabo dam model; hydrographs for these experiments are shown in Fig.4-9. Compared with case 1, the elapsed increased by 0.72 to 4.41 s, depending on the height of the sub-dam. The peak discharge was reduced by more than 82%. Sediment was deposited at the sub-dam, decreasing the concentration by 97%. The effects of the sub-dam were very similar to those observed in Cases 11–14 (SSF breaker and sub-dam). As in Case 14, we could not measure elapsed time, peak discharge, or concentration in Case 18.

For comparison, hydrographs of SSF for cases with only the sabo dam and SSF breaker are shown in Fig.4-10.

The effect of the experimental countermeasure structures is shown in Table 4-1 and Fig. 4-7~10. with changes on characteristic of SSF. The relationship between peak discharge and elapsed time is shown in Fig.4-11. The peak discharge was larger when there was less time for SSF to reach the bottom part of the flume. A comparison of Case 1 with Cases 2–10 shows the effect of the SSF breaker. In Case 2, SSF moved rapidly over the SSF breaker because there was no room for deposition; thus, peak discharge was large.

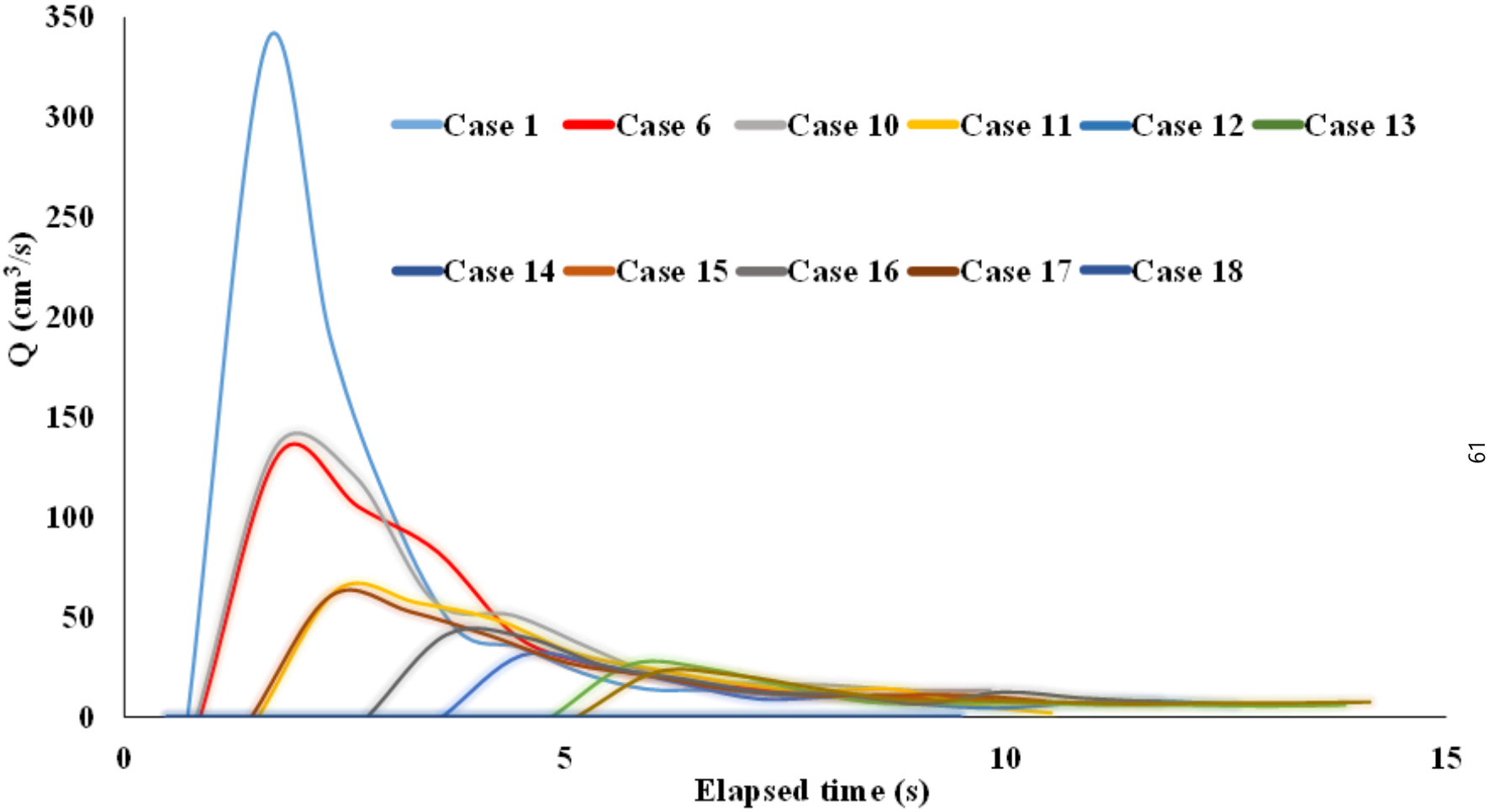

Fig. 4-10. Hydrograph of SSF (SD only and all cases with SSF breaker)

However, in Cases 3–10, peak discharge decreased by 50–60%. In Cases 11–18, SSF was trapped by the sub-dam, lengthening the elapsed time and reducing peak discharge by ≥80% by decreasing SSF velocity.

The relationship between sediment volume at the SSF breaker and sediment concentration is shown in Fig.4-12. In Cases 2–9, sediment volume at the breaker was affected by the breaker opening size. When larger amounts of sediment were deposited at the breaker, less sediment was discharged, thereby reducing sediment concentration. However, sediment concentration was larger in Case 2 than in Cases 3–6 because sediment overflowed the SSF breaker. In Cases 11–18, in which the SSF breaker opening size was the same as in Case 6, sediment concentration decreased by >90% because the sediment passing through the breaker was trapped by the sub-dam. When the concentration was 0%, all sediment and water passing through the SSF breaker was trapped by the sub-dam.

Results for Cases 11–18 are shown in Fig.4-13; these images were taken 60 s after the experiments. Due to the height of the sub-dam, it was difficult to determine the effect of the polymer in Cases 13, 14, 17, and 18. Although the gelation process took time, the effect of the polymer was confirmed for Cases 11, 12, 15, and 16. The red line indicates the height of sediment deposited at the sub-dam (side view).

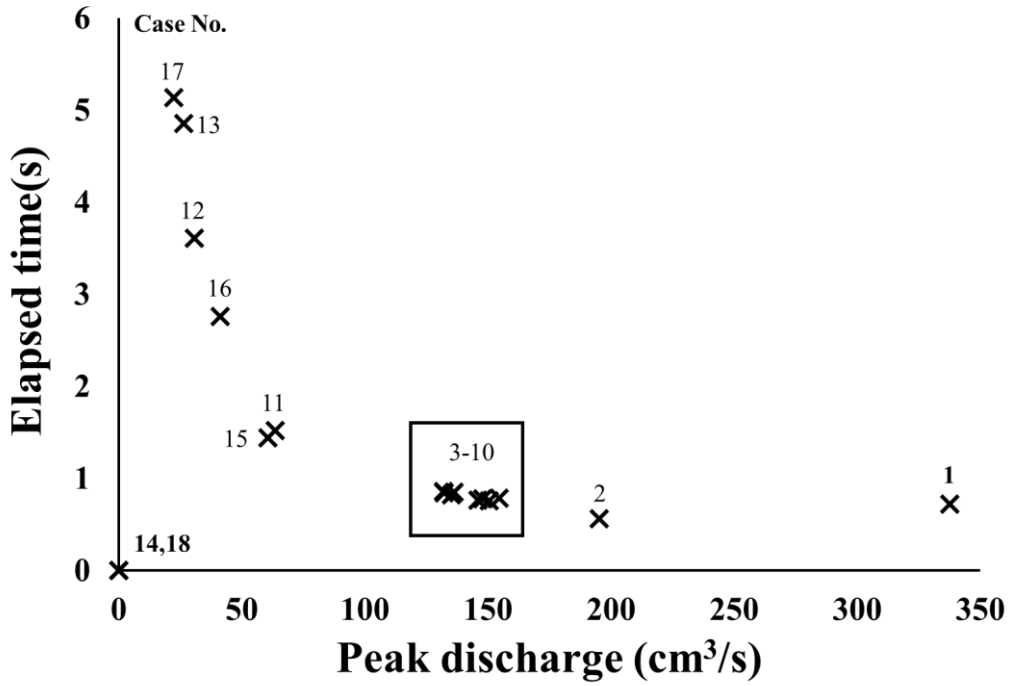

Fig. 4-11. Relationship between Elapsed time and Peak discharge

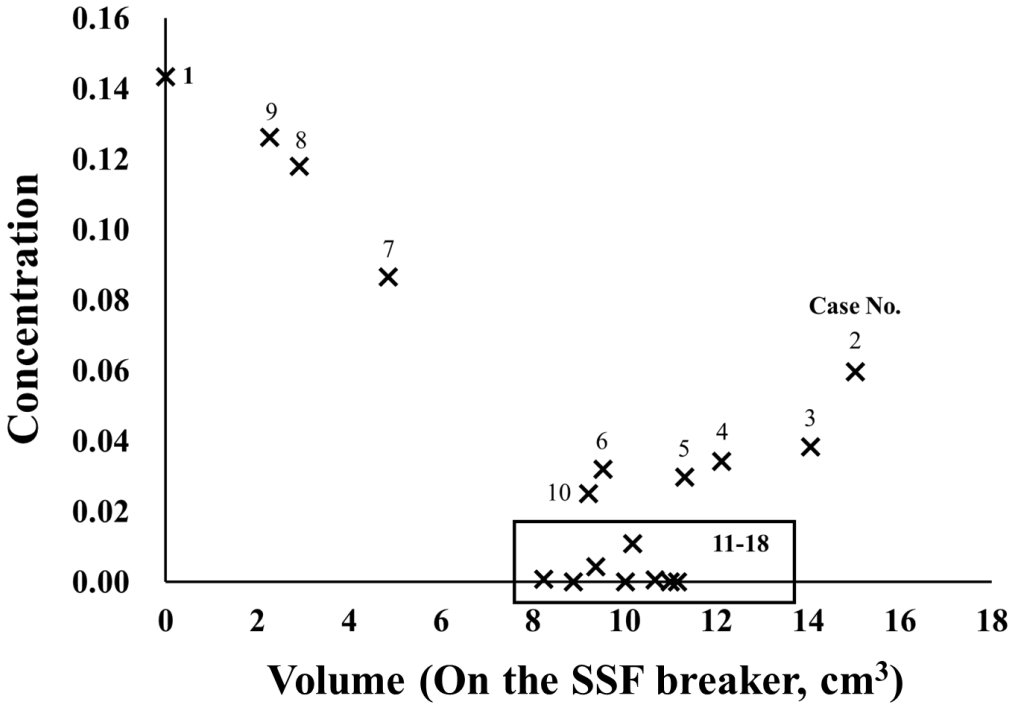

Fig. 4-12. Relationship between Concentration and Volume on the SSF breaker

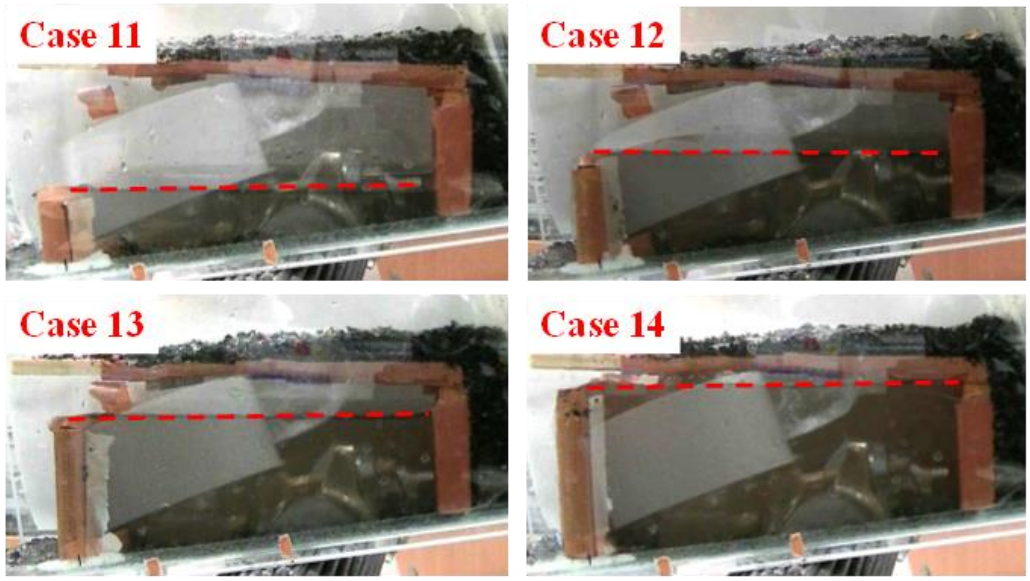

a. SD, SSF Breaker and Sub-dam

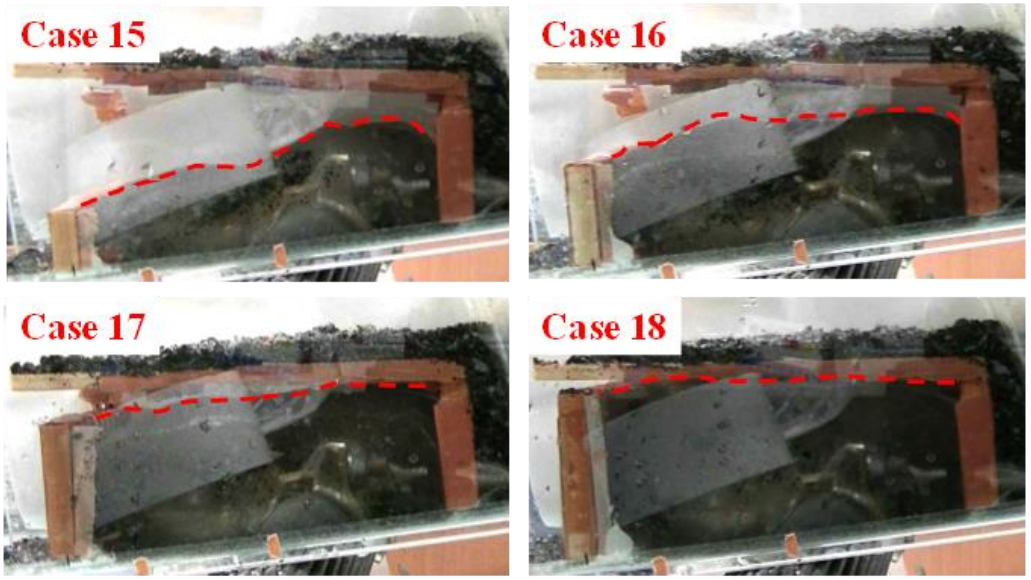

b. SD, SSF Breaker, Sub-dam and P(20)

Fig. 4-13. Results of deposition at bottom part (The red line depicts the deposition line)

4.4 Discussion

Installation of the SSF breaker increased the amount of deposition from SSF. The optimal SSF breaker opening size to decrease peak discharge was calculated as $d_{50(s)}/S_o$ = 0.54 for the flume conditions in this study. The SSF concentration was lowest in Case 5 ($d_{50(s)}/S_o$ = 1.08). Larger values of $d_{50(s)}/S_o$ were characteristic of SSF breaker overflow regardless of the amount of sediment deposited at the breaker. In such cases, sediment concentration was low, but peak discharge was high. Smaller values of $d_{50(s)}/S_o$ were predictive of SSF passing through the SSF breaker to the flume outlet, increasing peak discharge and concentration.

Table 4-2. Period of the polymer contact with water during experiment (in case 11, 12, 13, 15, 16 and 17)

Period of the polymer contact with water during experiment

Case No.	Case 11	Case 12	Case 13	Case 15	Case 16	Case 17
Height of Sub-dam (cm)	2.2	3.5	4.6	2.2	3.5	4.6
Period (s)	11.3	13.4	14.7	11.2	12.6	14.9

*Period means from the passing through the SSF breaker to finishing the outflow from the sub-dam

Under the conditions of our flume experiments, the amount of water contained in SSF was nearly 650 mL. It took about 50 s for the 20-g polymer to gelate the water in our simulated SSF (Fig.4-5). Despite the pool created by the sub-dam, very short periods were allowed for gelation by the polymer during our experiments (Table 4-2). Therefore, it was difficult to confirm the effectiveness of the polymer used in this study. However, the installation of the SSF breaker and sub-dam at the sabo dam in our flume model decreased both peak discharge and SSF concentration, especially when the height of the sub-dam was large.

4.5 Conclusion

In this chapter, we conducted flume experiments to determine how installing an SSF breaker, polymer, and sub-dam downstream of a sabo dam would affect SSF. We determined that the optimal value of $d_{50(s)}/S_o$ was 0.54 to decrease peak discharge and SSF concentration under the conditions of these experiments. The installation of the SSF breaker decreased peak discharge and SSF concentration; the addition of a sub-dam considerably enhanced these effects, especially when the height of the sub-dam was large due to its greater ability to trap sediment.

Future studies should conduct detailed investigation of water-absorbing polymers in the field, as small-scale experiments do not allow sufficient time for water gelation. Controlling the amount of water in SSF is important for mitigating damage in SSF-related disasters. The amount and grain size of supplied sediment should also be varied to obtain empirical data applicable to further field studies.

Chapter 5

Experimental study on physical measures against subsequent sediment flow

(SSF breaker, 2nd SSF breaker, polymer, and sub-dam)

5.1 Introduction

In the result of Chapter 4, even though the effect of polymer was not known much, it was found that the experimental countermeasure structures (SD, SSF breaker, polymer, and sub–dam) reduced the peak discharge, concentration, and hydrograph of SSF to be effective in mitigate SSF. However, the amount of SSF is fixed in the flume experiment. The amount of the SSF in the field may less or much than in the flume experiment. Therefore if there is much amount of the SSF, the sediment may overflow at the field even if all of the sediment has been completely been controlled in case 13, 14 and case 17, 18 of Chapter 4 in the experiment. Also, when the height of sub–dam is 2.6 cm and 3.8 cm (in cases 11, 12, 15, and 16), it is necessary to research how to control sediment further, since it is small in amount but sediment was outflowed. Because even these small amount of sediment also can be given a damage to residential area in the field. In this Chapter, besides the experimental countermeasure structures (SSF breaker, polymer, and sub–dam) which suggested in Chapter 4, the flume experiment was conducted by adding 2nd SSF breaker attach to sub–dam.

The purpose of adding the 2nd SSF breaker is to reduce the amount of sediment by catchment of the SSF which is after passed through the SSF breaker. In Chapter 4, the SSF was reduced greatly by installing experimental countermeasure structures, but when the height of sub-dam was 2.2, 3.5, and 4.6 cm, SSF flowing was checked. This flume experiment performed to figure out the effect of 2nd SSF breaker to concentration and discharge of the SSF. The interval of the 2nd SSF breaker was determined as the D_{50} of 2nd SSF, in order to control over the half of sediment in the 2nd SSF.

5.2 Method

Fig. 5-1 shows the experimental conditions. Condition of experimental flume and the amount of supplied sediment and water are the same with the condition of chapter 4. Also Experimental countermeasure structures are identical with chapter 4 except 2nd SSF breaker (12 cm long and 7.5 cm width). 2nd SSF breaker made by stainless wire mesh (the interval of wire mesh: 0.6 mm, Wire diameter: 250 μm, Open area: 45%). The interval of wire mesh was determined to catchment approximately 50 % of sediment in the SSF. Fig. 5-2 shows the grain size distribution of the SSF which dropped from SSF breaker.

All experiments were performed on new 6 cases (case 19 ~ 24) and the values of case 1, 11, 12, 13, 15, 16, and 17 used for comparing with the results of this flume experiment (Table 5-1). Case 14 and 18 (the height of sub–dam: 5.8 cm) were ruled out because all amount of the SSF was trapped by sub–dam. Case 19, 20, 21 and 22, 23, 24 were divided by the height of sub–dam, and existence and nonexistence of 2nd SSF breaker. Elapsed time, peak discharge, and concentration were measured throughout the experiments as the same way with Chapter 4.

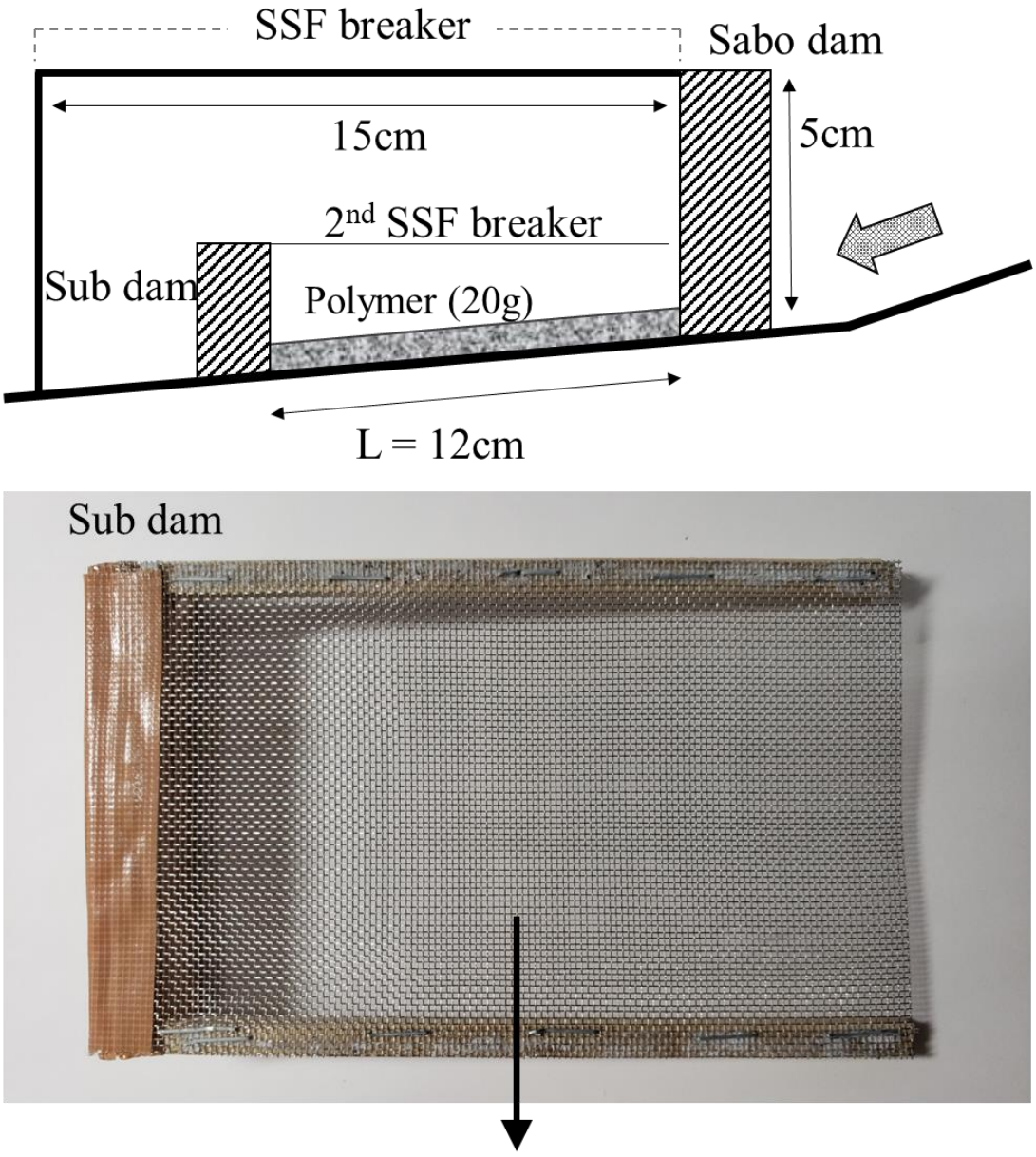

Fig. 5-1. Sketch of 2nd SSF breaker

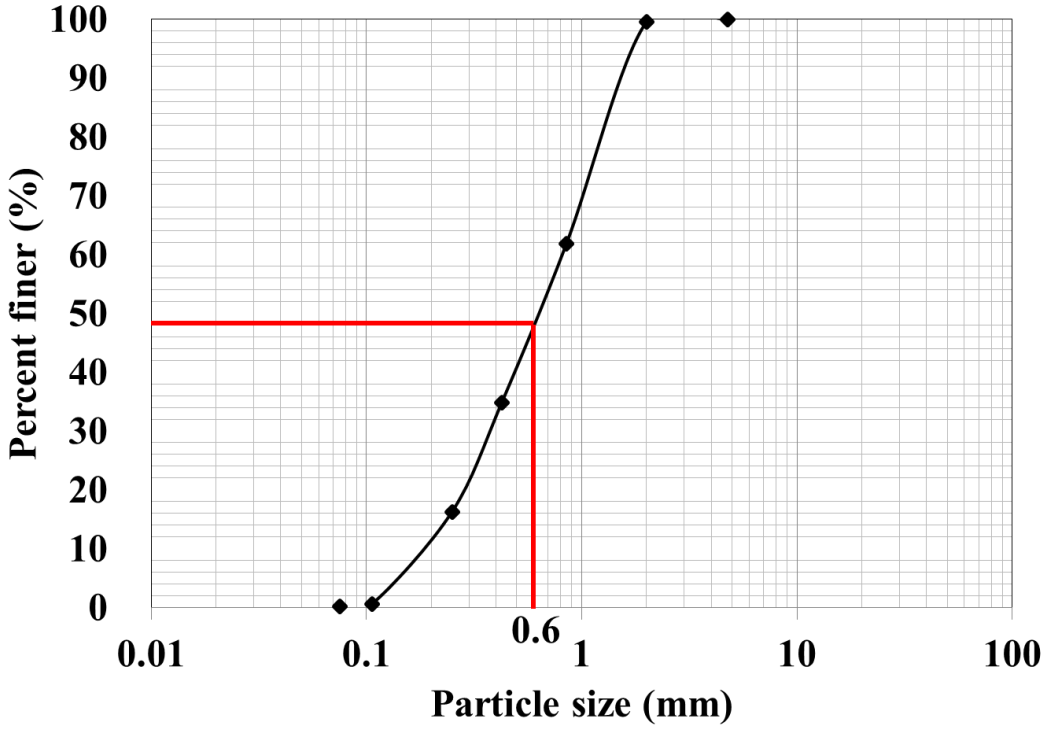

Fig. 5-2. Grain size distribution of SSF

5.3 Result

The results of flume experiment are shown in Table 5-1.

Table 5-1. Experimental cases and result values of each case (with 2nd SSF breaker)

	Case	Sub dam$_h$	Elapsed time(s)	C	Q_p (cm^3/s)
SD	Case1		0.72	0.1434	337.6500
SD + SSF breaker + Sub-dam	Case11	2.2	1.52	0.0108	63.63
	Case12	3.5	3.61	0.0008	30.82
	Case13	4.6	4.85	0.0000	26.35
SD + SSF breaker + P(20) + Sub-dam	Case15	2.2	1.44	0.0043	60.64
	Case16	3.5	2.76	0.0005	41.26
	Case17	4.6	5.13	0.0000	22.37
SD + SSF breaker + Sub-dam + 2nd SSF breaker	Case19	2.2	1.50	0.0073	61.64
	Case20	3.5	2.95	0.0002	30.82
	Case21	4.6	4.30	0.0000	16.90
SD + SSF breaker + P(20) + Sub-dam + 2nd SSF breaker	Case22	2.2	1.53	0.0027	58.66
	Case23	3.5	2.55	0.0001	28.83
	Case24	4.6	5.90	0.0000	15.91

5.3.1 Effect of 2nd SSF breaker

In order to clear the effect of 2nd SSF breaker, experimental cases were compared; case 15 to 17, and case 22 to 24 (Fig. 5-3). Hydrographs were divided by each case of the same height of the sub-dam. The difference of peak discharge of SSF could be confirmed as set experimental countermeasure structures. Also, values of concentration showed differ in each case, but it was too low to figure out the effect of 2nd SSF breaker.

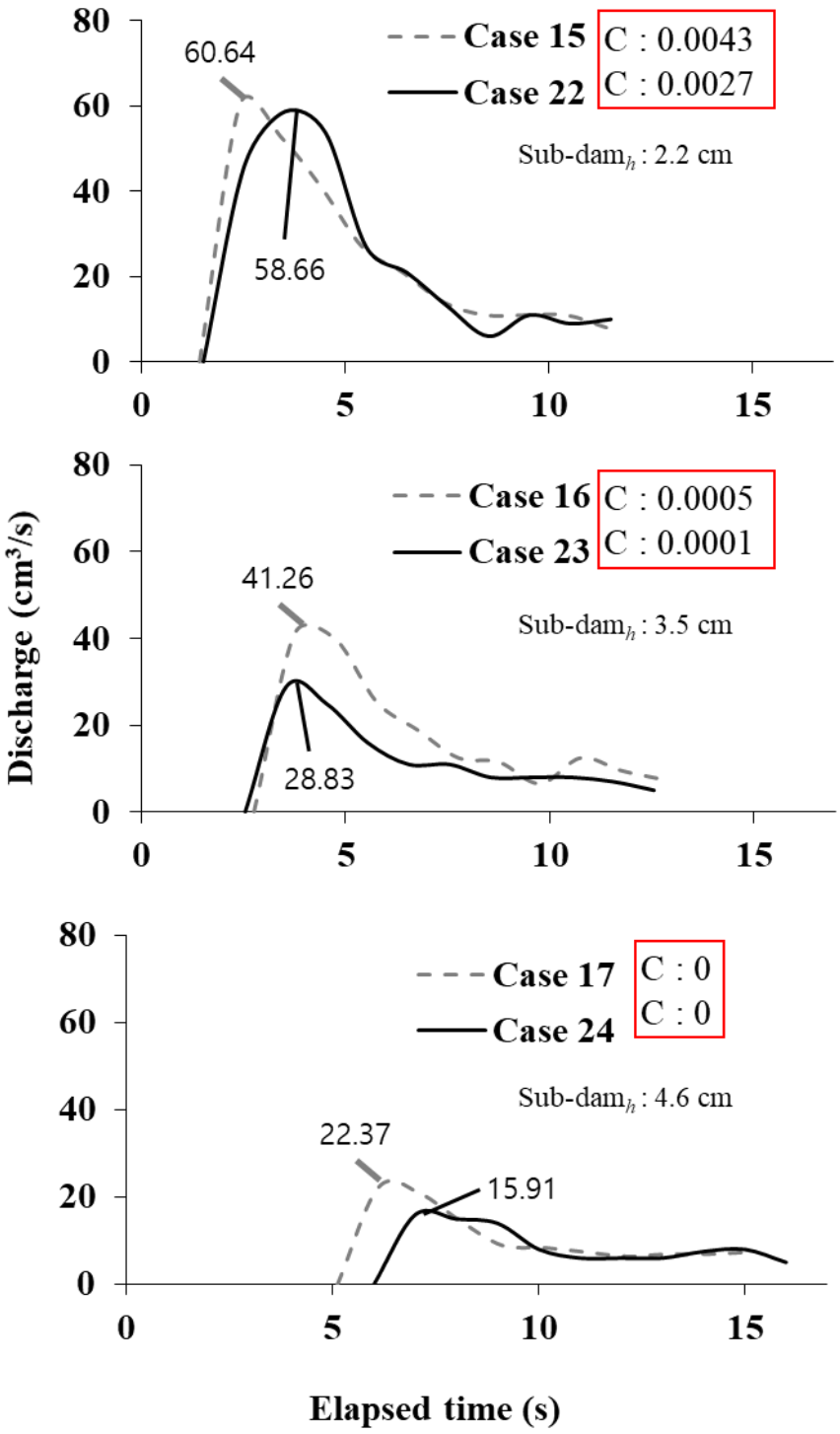

Fig. 5-3. Hydrographs of SSF (Case 15 to 17, and case 22 to 24)

Compare to cases of with/without 2nd SSF breaker, peak discharge and concentration were slight reduced by trapping the sediment by 2nd SSF breaker (Fig. 5-4). When SSF fall down from SSF breaker, sediment of SSF was trapped by 2nd SSF breaker. As sediment is trapped by 2nd SSF breaker, sub-dam can store more water for a while as sediment volume. It means, the function of 2nd SSF breaker increases the storage capacity of sub-dam for a while.

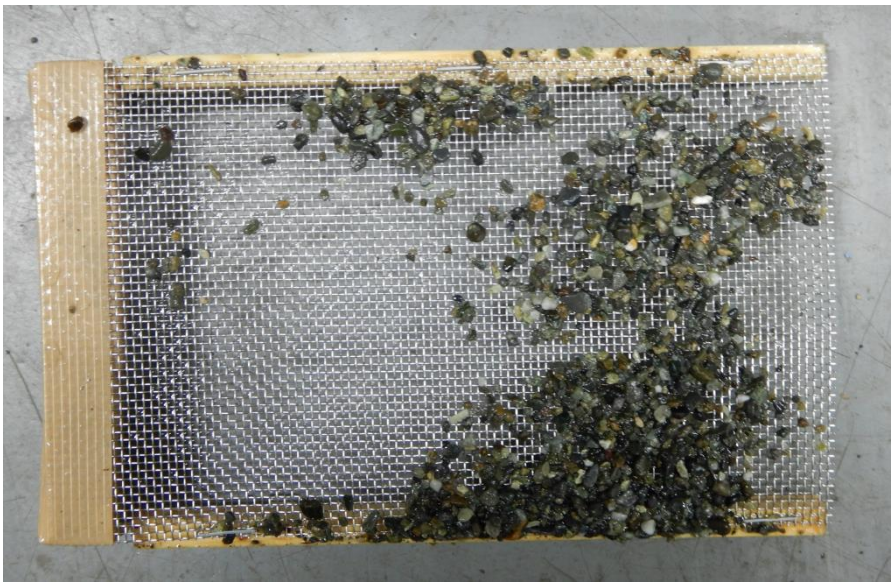

Fig. 5-4. Trapped sediment by 2nd SSF breaker

5.3.2 Effect of Polymer

In order to figure out the function of polymer in the experimental cases, we compared with Fig. 5-3 and Fig 5-5. With the results, function of SSF breaker, 2nd SSF breaker and sub-dam could be figure out. But the function of polymer was not clear in the condition of flume experiments.

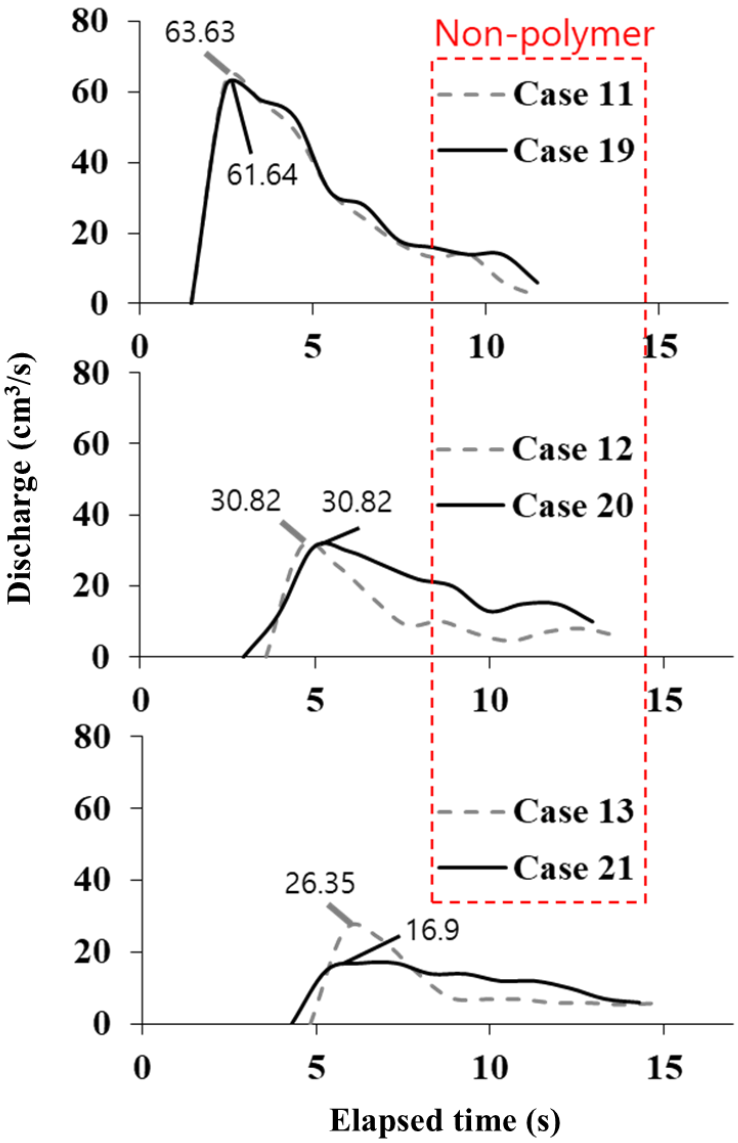

Fig. 5-5. Hydrographs of SSF (Case 11 to 13, and case 19 to 21)

Fig. 5-6 shows the relationship among the Elapsed time, Peak discharge and concentration. As same as the results of Chapter 4, Elapsed time was delayed according to the height of the sub-dam. The result of peak discharge also cannot explain certainly which side is more effective. But concentration had difference as with/without 2nd SSF breaker. This result shows the sediment catchment effect of 2nd SSF breaker.

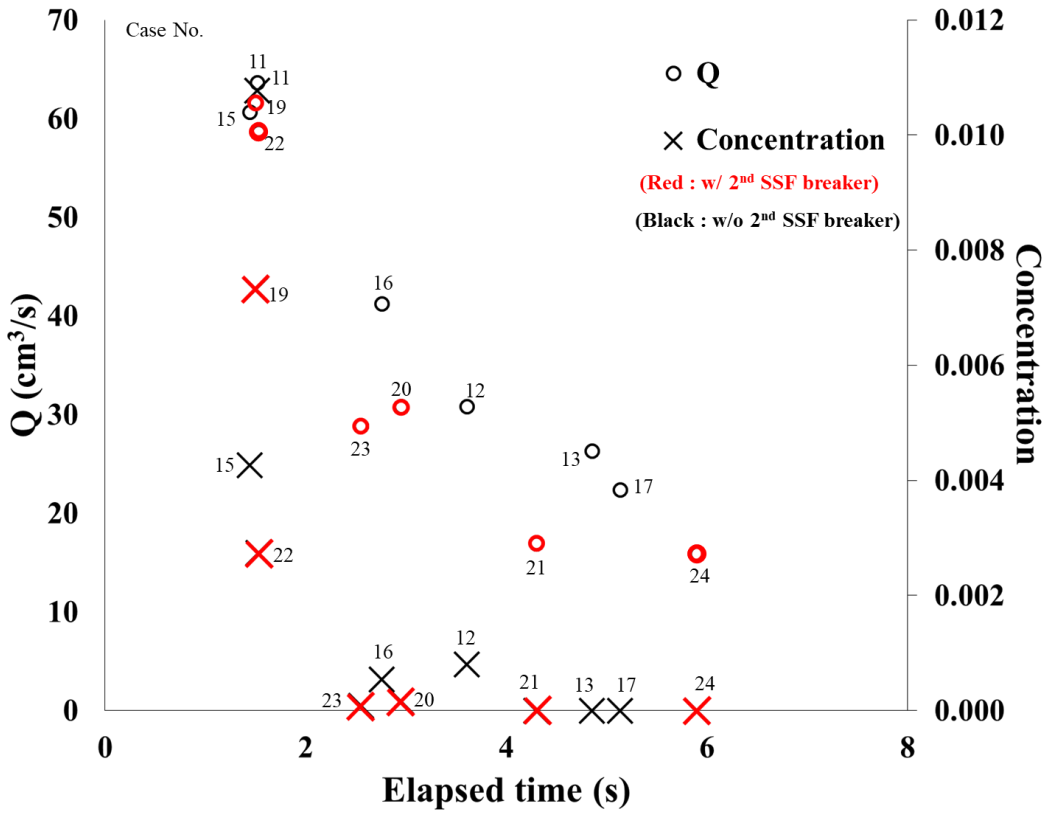

Fig. 5-6. Relation among the peak discharge, concentration and elapsed time

5.4 Discussion

Even though Peak discharge and concentration of SSF were already decreased greatly in Chapter 4 (over 81 % in peak discharge and 92 % in concentration), installed 2nd SSF breaker on sub-dam to increase trapping effect the sediment of 2nd SSF.

It was confirmed that the 2nd SSF breaker could trap the sediment of 2nd SSF effectively through the experiment. With the results in Table 5-1, it is shown that the concentration and discharge of SSF in case 19 to 24 with 2nd SSF breaker have effectively decreased though small value (compare with case 11 to 17; concentration: 32 ~ 85%, discharge: 0.03 ~ 0.3%). It considered that the sediment was trapped by 2nd SSF breaker and affected the amount of discharge.

Also in Chapter 5, the effect of polymer could not find. As the same opinion with chapter 4, it considered that took more time to gelation in dynamic condition.

In order to confirm the expected effect of field application of SSF countermeasures structures verified through the flume experiment, the hydrodynamic force and discharge of the SSF occurred in Hiroshima were used. Among the experimental cases, the hydrodynamic force and discharge of Case 1 were considered to the same values as study sites. If SSF occurs again with the same condition of Hiroshima, it would be expected to reduce 98.6% of hydrodynamic force and 95.3% of discharge (Case 24) when all the proposed SSF countermeasure structures had been constructed (Fig.5-7).

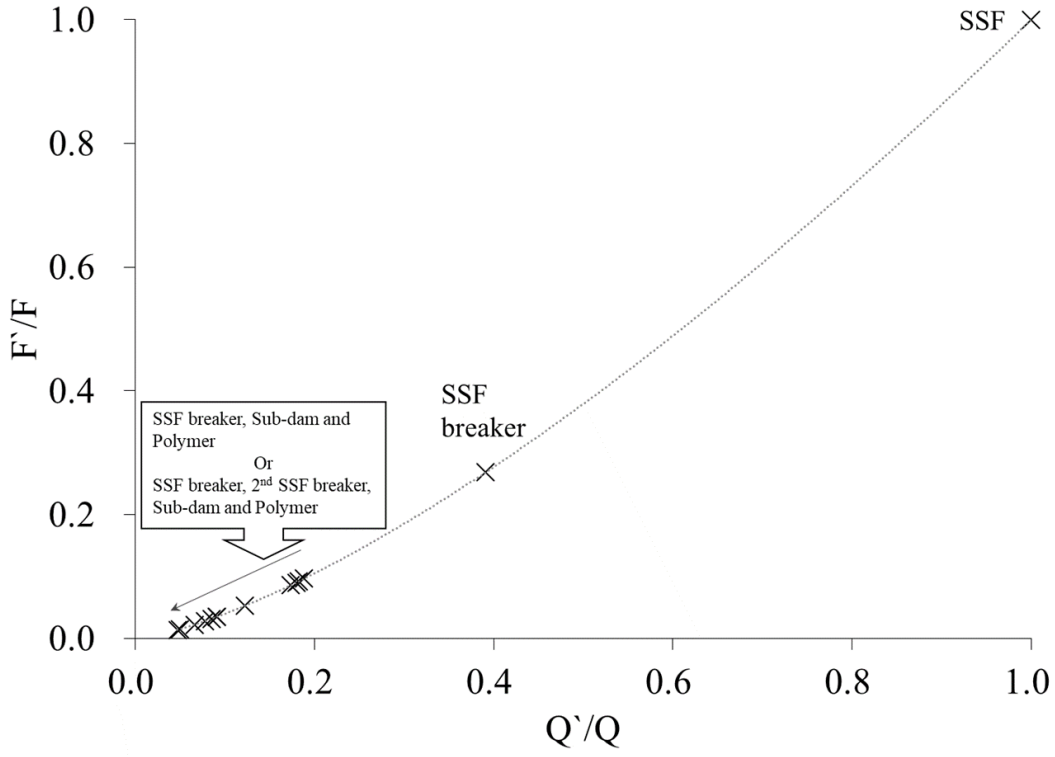

Fig. 5-7. Relation of hydrodynamic force and discharge of SSF

5.5 Conclusion

In this chapter, flume experiments were conducted to confirm the effect of 2nd SSF breaker to mitigate the SSF. The concentration was decreased as trap the sediment of 2nd SSF by 2nd SSF breaker. As sediment trapped in SSF by 2nd SSF breaker then discharge of SSF also reduce. Therefore it might help to mitigate SSF.

While the experimental study has small result values due to small scale, it is expected that the effect will be large when apply to the field with large scale according to the existence and nonexistence of 2nd SSF breaker. Though more research needed on polymer, with this experiment, SD, SSF breaker, 2nd SSF breaker, polymer, and sub-dam are confirmed that effective in mitigate SSF under experimental study condition.

In the future, more experimental studies of various cases will be required to be applied in the field. Various gradients, widths, grain sizes, and amount of sediment should be considered. Also, future research is needed on polymer. It is important to control both sediment and water for mitigating the SSF effectively.

Chapter 6

General Conclusion

This dissertation aims to propose a novel SSF countermeasure for installation at sabo facilities upstream of high population density areas. Under these objectives, the actual situation of area damaged from SSF was surveyed to understand insufficient of countermeasure facilities against SSF to high population density areas. And the flume experiment was conducted to clear the effect of experimental countermeasure structures mitigate SSF by using SSF breaker, polymer, sub-dam, and 2nd SSF breaker.

Actual situations of damage from SSF were confirmed through field survey; sediment inflows to houses, parking lots, and gardens, and where glass was broken. These damages were occurred by insufficient of SSF countermeasure facilities due to lack of space. Because the residential areas were located in downstream. Hydrodynamic force was calculated based on survey data, and damage degree was figured out from hydrodynamic force. These results shows the necessity of novel countermeasure facilities against the SSF to reduce the damage from SSF in high population density area. We proposed novel countermeasure facilities against the SSF through the performance of flume experiments.

The Flume experiments were conducted in order to clear the effectiveness of SSF countermeasure facilities.

1. SD, SSF breaker, Polymer, and Sub-dam

   Due to installation of the SSF breaker on SD and by adding the sub-dam on the experimental flume, the peak discharge and concentration of the SSF were greatly decreased. Separate the sediment and water by SSF breaker first, and the sub-dam trap the SSF at the under the SSF breaker. Discharge of outflow was expected to reduce further as water from the SSF trapped by Sub-dam to be absorbed by the polymer, but the effect of the polymer was not confirmed clearly.

2. SD, SSF breaker, Polymer, Sub-dam, and 2nd SSF breaker

Compare with non-2nd SSF breaker condition, peak discharge was decreased, and also concentration was reduced but slight. Concentration is decreased enough even in the non-2nd SSF breaker condition, 2nd SSF breaker is effective to decrease peak discharge of SSF. 2nd SSF breaker increases the storage capacity of sub-dam for a while as sediment volume which trapped.

The experimental results of chapters 4 and 5 confirmed that the novel SSF countermeasure proposed in this experiment can reduce the sediment concentration and peak discharge of SSF, also make a lower hydrograph of SSF. When the ratio of mean grain size and opening size of the SSF breaker is 0.54 ~ 1.08, it is the most effective to mitigate the SSF. As a result, it is expected that the extent of flooding and sedimentation of the SSF in high population density areas can be reduced, and damage to house, especially the damage caused by sediment and water intrusion into house due to the destruction of opening can be reduced.

However, this study is just the indoor experiment step so far. There are some considerations to be considered in order to apply to the field. Because the amount of the SSF varies depending on the amount of the debris flow, so changes in the SSF countermeasure structures proposed in the study are necessary to suitable for the field.

1. Amount of SSF

In the flume experiment, the amount of supplied sediment was determined according to the sediment volume at the full deposition condition of the SD. Since the amount of supplied sediment and water was fixed, in chapters 4 and 5, the SSF countermeasure structures mitigated SSF greatly or trapped the whole

of SSF. However, due to the amount of SSF depends on the amount of debris flow in the field, it is important to predict the amount of outflow sediment in debris flow from the drainage basin area when constructing the SSF countermeasure structures.

2. Condition of drainage basin

The condition of each drainage basin (amount of rainfall, sediment volume, gradient, grain size, and etc.) is different, therefore the characteristics of the runoff sediment are also different depending on the characteristics of the basin. As grain size and discharge of SSF, not only interval of SSF breaker and 2nd SSF breaker but also scale of SSF breaker, 2nd SSF breaker, and sub-dam be decided. Therefore the amount and grain size of supplied sediment need to be varied to obtain data applicable to field work.

Also, if the left and right side stratum of SD downward is weak, there is a possibility to outflow with SSF to downstream after slope failure of stratum. It makes more damage to downstream. In such cases, installation of side SSF breaker might helpful to mitigate SSF [*Yokota et al.*, 2012; *Kim et al.*, 2017] (Fig. 6-1).

3. Polymer

Debris flow is most often caused by torrential rainfall but the flume experiments were not a rainy condition. Therefore the polymer first comes into contact with water when the SSF occurs. However, in the field, if the polymer is placed as in the flume experiment, the water will be absorbed first by the rainfall. For this reason, in order to apply in the field, it is necessary to make a facility to function

after the occurrence of SSF.

In the flume experiment, the function of the polymer was not clear. However, the control of the sediment is important, but it is necessary to control the water to further mitigate the SSF. Therefore more research is needed to effectively use the polymer.

Fig. 6-1. Debris breaker with side breaker
(*Brunkal and Santi*, 2016)

If SSF countermeasure facilities are installed on high population density area, generally the construction of sabo dam and SSF countermeasure facilities is duty of government. Therefore it will be easier and less costly to do the homeowner's defense work if it needs (e.g. wooden deflector, engineered concrete block wall, sandbag stacking against buildings, etc) [*Los Angeles County*, 2018] (Fig. 6-2). It is necessary to supplement points to be supplemented through continuous monitoring for being effective on the field. Also, recently, sediment and flood damage has been a problem in Japan. The countermeasure facilities proposed in this study could be developed as a countermeasure against sediment and flood damage at the exit of the valley as well as SSF.

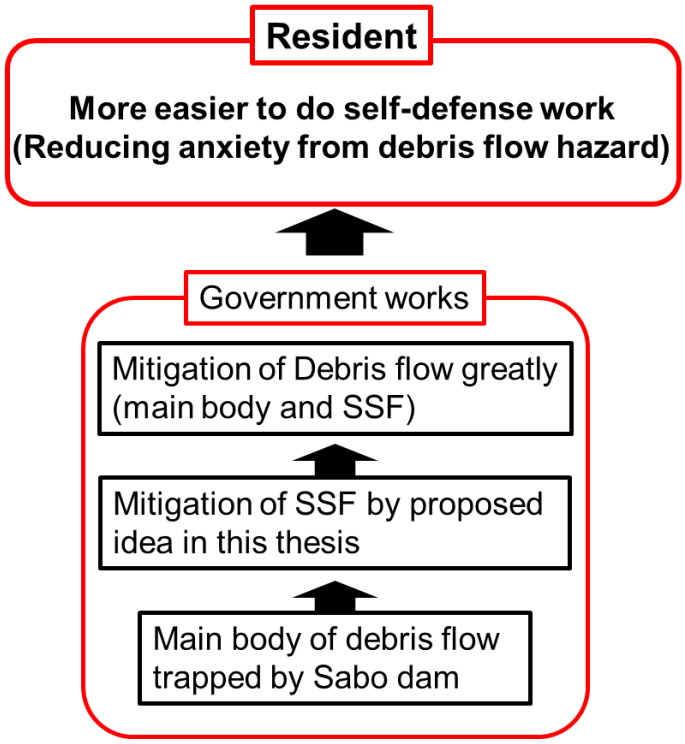

Fig. 6-2. Effect expectation of SSF countermeasure facilities

References

Arai, M., Takahashi, T. and Kato, C. (1997): Effect on particle size by controlling of debris flow by absorbent polymer, Proceeding of 2nd Annual conference of JSCE, No. 52, pp. 466-467 (in Japanese).

Brighenti, R., Segalini, A. and Ferrero, A.M. (2013): Debris flow hazard mitigation: A simplified analytical model for the design of flexible barriers, Computers and Geotechnics, Vol. 54, pp. 1-15.

Brunkal, H. and Santi, P. (2016): Exploration of design parameters for a dewatering structure for debris flow mitigation. Engineering Geology 208, pp. 81-92.

Cho, S., Yoo, B., Kim, J. and Lee, K. (2016): Performance assessment for debris mitigation structure by using scale model tests. J. Korean Soc. Hazard Mitig. Vol. 16, No. 5, pp. 247-260.

Cui, P., Zeng, C. and Lei, Y. (2015): Experimental analysis on the impact force of viscous debris flow. Earth Surf. Process. Landforms 40, 1644-1655.

Dahal, R. K., Hasegawa, S., Nonomura, A., Yamanaka, M., Masuda, T. and Nishino, K. (2009): Failure characteristics of rainfall-induced shallow landslides in granitic terrains of Shikoku Island of Japan, Environ. Geol., No. 56, pp. 1295–1310.

Doshida, S. and Araiba, K. (2015): The geographicaeatures of the hiroshima landslide disaster triggered by heavy rainfall on august 20, 2014. 10th Asian regional conference of IAEG.

Gonda, Y. (2009): Function of a debris-flow brake, International Journal of Erosion Control Engineering, Vol. 2, No. 1, pp. 15-21.

Handa, R. and Yamada, T. (2011): Damage characteristics of houses in the subsequent sediment flow prone area, Proceeding of 60th Annual conference of JSECE, pp. 558-559 (in Japanese).

Hiroshima Prefecture (2018): Disaster by torrential rainfall in July 2018, Report from Disaster countermeasure office of Hiroshima prefecture, No. 51.

Hubl, J., Fiebiger, G., Jakob, M. and Hungr, O. (2005): Debris-flow mitigation measures,

ICHARM. (2008): Debris-flow dewatering brakes: a promising tool for disaster management in developing countries, International Center for Water Hazard and Risk Management Newsletter, Vol. 3, No. 3, pp. 10.

Imai, K., Miyamoto, N. and Mizuyama, T. (1989): Test of a debris flow breaker at the Kamikamihori valley, Mt. Yakedake (Part-2), Journal of the Japan Society of Erosion Control Engineering, Vol. 42, No. 2 (163), pp. 16-20 (in Japanese).

Irasawa M. and Shimohigashi H. (1988): Study of disaster prevention with a sabo dam, Journal of the Japan Society of Erosion Control Engineering, Vol. 41, No. 3 (158), pp. 11-16 (in Japanese).

Iverson, R.M. (1997): The physic of debris flows, Reviews of Geophysics, Vol. 35, No. 3, pp. 245-296.

Iverson, R.M. (2015): Scaling and design of landslide and debris-flow experiments, Geomorphology, 244, pp. 9-20.

Jeong, S.S., Kim, Y.M., Lee, J.K. and Kim, J.H. (2015): The 27 july 2011 debris flows at Umyeonsan, Seoul, Korea, Landslides.

JSECE (2015): Suggestion based on emergency survey by Japan Society of Erosion Control Engineering of Large-scale debris flow disaster in Hiroshima. Journal of the Japan Society of Erosion Control Engineering, Vol. 68, No. 1, pp. 103-105 (in

Japanese).

Kasai, H. (1980): A review of investigations on mudflow (I). -On the conception and conditions of occurrence of mudflow-, Japan Society of engineering Geology, Vol. 21, No. 3, pp.132-144.

Kasim, N., Taib, K.A., Mukhlisin, M. and Kasa, A. (2016): Triggering mechanism and characteristic of debris flow in peninsular Malaysia. American journal of engineering research, Vol. 5, No. 4, pp. 112-119.

Kim, J.H., Chun, K.W., Seo, J.I., Kim, S.W., Yun, J.U. and Jun, K.W. (2016): An examination of optimum slit aperture suited to flat-board debris-flow breaker in residential piedmont areas, Crisisonomy, Vol. 12, No. 4, pp. 73-83 (in Korean).

Kim, J.H., Chun, K.W., Seo, J.I., Lee, Y.T. and Jun, K.W. (2017): The effect of side screen attached to flat-board breaker on damage reduction, Crisisonomy, Vol. 13, No. 1, pp. 109-121 (in Korean).

Kiyono M., Miyakoshi H., Uehara S. and Mizuyama T. (1986): Test of a debris-flow brake in Kamikami valley, Mt.Yake-dake, Journal of the Japan Society of Erosion Control Engineering, Vol. 39, No. 3 (146), pp. 15-19 (in Japanese).

Kurihara, J., Mizuyama, T. and Suzuki, H. (1989): Effect on controlling the debris flow by absorbent polymer, Proceeding of 38th Annual conference of JSECE, pp. 161-164 (in Japanese).

Los Angeles public works (2018): Homeowner's guide; for flood, debris, and erosion control.

Marchi, L., Comiti, F., Crema, S. and Cavalli, M. (2019): Channel control works and sediment connectivity in the European Alps, Science of the total environment 668, pp. 389-399.

Miwa, K. and Taketoshi, K. (2018): Emergency responses to debris flow disaster at serizawa district, nikko city triggered bt the 2015 torrential rains in the kanto and tohoku region, Symposium Proceedings of the Interpraevent 2018 in the Pacific Rim, pp. 153-162.

Mizuyama, T. (1980): Sediment transport rate in the transition region between debris flow and bed load transport, Journal of erosion control engineering, Vol. 33, No. 1, pp. 1-6.

Mizuyama, T. (2008): Structural countermeasures for debris flow disasters. International Journal of erosion control engineering, Vol. 1, No. 2, pp. 38-43.

Mizuyama, T., Nakano, M. and Nanba, A. (1998): Case study on debris flow control. Journal of the Japan Society of Erosion Control Engineering, Vol. 51, No. 4, pp. 36-39 (in Japanese with English abstract).

NILIM (2016): Manual of Technical Standard for establishing Sabo master plan for debris flow and driftwood, Technical note of National Institute for Land and Infrastructure Management, No.904 (In Japanese with English abstract)

Ohkubo, S., Fukui, N., Mizuyama, T. and Sugasaki, M. (1988): Analysis of sediment discharge control with sabo dams, Journal of the Japan Society of Erosion Control Engineering, Vol. 41, No. 4 (159), pp. 21-25 (in Japanese).

Pierson, T.C. (2005): Distinguishing between debris flows and floods from field evidence in small watersheds, USGS Fact Sheet, 2004-3142.

Senoo, K., Mizuyama, T. and Uehara, S. (1983): Experimental study on checking of debris flous with sabo dams, Journal of the Japan Society of Erosion Control Engineering, Vol. 36, No. 2 (129), pp. 17-23 (in Japanese with English abstract).

Shrestha, B.B., Nakagawa, H., Kawaike, K. and Baba, Y. (2008): Numerical simulation on debris-flow deposition and erosion processes upstream of a check dam with

experimental verification. Annuals of Disas. Prev. Res. Inst., Kyoto Univ., No. 51 B, pp.613-624.

Song, D., Choi, C.E., Zhou, G.G.D., Kwan, J.S.H. and Sze, H.Y. (2018): Impulse load characteristics of boulder debris flow impact, Geotechnique letters 8, 111-117.

Takahara, T. and Matsumura, K. (2008): Experimental study of the sediment trap effect of steel grid-type sabo dams. International Journal of erosion control engineering, Vol. 1, No. 2, pp. 73-78.

Takahashi, T., Nakagawa, H., Satofuka, Y. and Kawaike, K. (2001): Flood and sediment disasters triggered by 1999 rainfall in Venezuela. A river restoration plan for an alluvial fan, Journal of Natural Disaster Science, Vol. 23, No. 2, pp. 65-82.

Volkwein, A., Wendeler, C. and Guasti, G. (2011): Design of flexible debris flow barriers. Italian Journal of Engineering Geology and Environment.

Watanabe, M., Mizuyama, T. and Uehara, S. (1980): Review of debris flow countermeasure facilities, Journal of the Japan Society of Erosion Control Engineering, Vol. 32, No. 4, pp. 40-45 (in Japanese).

Xie, T., Wei, F., Yang, H., Gardner, J.S. and Xie, X. (2017): A design method for a debris flow water-sediment separation structure. Eng. Geol. 220, pp. 94–98.

Xie, T., Yang, H., Wei, F., Gardner, JS., Dai, Z. and Xie, X. (2014): A new watersediment separation structure for debris flow defense and its model test. Bull Eng Geol Environ, Vol. 73, No. 4, pp. 947–958.

Yamamoto, A., Yamamoto, S., Toriihara, M. and Hirama, K. (1998): Impact load on sabo dam due to debris flow, Journal of the Japan Society of Erosion Control Engineering, Vol. 51, No. 2, pp. 22-30 (in Japanese with English abstract).

Yokota, M., Yoshida, K., Furuyama, T. and Handa, K. (2012): Motion analysis of debris

flows monitored on the float-board debris-flow breaker, Journal of erosion control engineering, Vol. 65, No. 4, pp. 45-49.

Zeng, C., Cui, P., Su, Z., Lei, Y. and Chen, R. (2015): Failure modes of reinforced concrete columns of buildings under debris flow impact, Landslides 13, No. 3, pp. 561-571.

Publications and academic conferences

1) Publication

Kim, Y, Takashi, Y. (Accepted). Experimental study of sabo dam physical measures against subsequent sediment flow following debris flow deposition. International Journal of erosion control engineering.

2) Academic conferences

Kim Yong Rae, Tomomi Marutani, Mio Kasai and Sinya Katsura. Flume experiment of debris flow mitigation applying water absorbent and screen dam model. Symposium of Japan Society of Erosion Control Engineering, May 18-20, 2016, Toyama, Japan (Oral presentation).

Yong Rae Kim, Yamada Takashi. The effect of polymer on the change in the hydrograph of the successive debris flow. Symposium of Japan Society of Erosion Control Engineering, May 16-18, 2018, Yonago, Japan (Poster presentation)

Yong Rae Kim, Yamada Takashi. Experimental study of countermeasures against the successive debris flow. International Symposium INTERPRAEVENT, Oct 1-4, 2018, Toyama, Japan (Poster presentation)